FIRAT UNIVERSITY
GRADUATE SCHOOL OF NATURAL AND APPLIED SCIENCES
TÜRKİYE

INVESTIGATION OF MICROSTRUCTURE AND THERMODYNAMIC PROPERTIES OF NiTiCu SHAPE MEMORY ALLOY AGED AT DIFFERENT TEMPERATURES

Azad Ibrahim HAJI

Master's Thesis

DEPARTMENT OF PHYSICS

Division of General Physics

MAY 2021

FIRAT UNIVERSITY
GRADUATE SCHOOL OF NATURAL AND APPLIED SCIENCES
TÜRKİYE

Department of Physics

Master's Thesis

INVESTIGATION OF MICROSTRUCTURE AND THERMODYNAMIC PROPERTIES OF NiTiCu SHAPE MEMORY ALLOY AGED AT DIFFERENT TEMPERATURES

Author
Azad Ibrahim HAJI

Supervisor
Prof. Dr. Cengiz TATAR

MAY 2021
ELAZIG

FIRAT UNIVERSITY
GRADUATE SCHOOL OF NATURAL AND APPLIED SCIENCES

TÜRKİYE

Department of Physics

Master's Thesis

Title:	Investigation of Microstructure and Thermodynamic Properties of NiTiCu Shape Memory Alloy Aged at Different Temperatures
Author:	Azad Ibrahim HAJI
Submission Date:	26 April 2021
Defense Date:	25 May 2021

THESIS APPROVAL

This thesis, which was prepared according to the thesis writing rules of the Graduate School of Natural and Applied Sciences, Fırat University, was evaluated by the committee members who have signed the following signatures and was unanimously approved after the defense exam made open to the academic audience.

		Signature
Supervisor:	Prof. Dr. Cengiz TATAR Firat University, Faculty of Science	Approved
Chair:	Title Name SURNAME ... University, Faculty of	Approved
Member:	Title Name SURNAME ... University, Faculty of	Approved
Member:	Title Name SURNAME ... University, Faculty of	Approved

This thesis was approved by the Administrative Board of the Graduate School on

..... / ..... / 20 .....

Signature

Assoc. Prof. Dr. Kursat Esat ALYAMAÇ
Director of the Graduate School

DECLARATION

I hereby declare that I wrote this Master's Thesis titled “Investigation of Microstructure and Thermodynamic Properties of NiTiCu Shape Memory Alloy Aged at Different Temperatures” in consistent with the thesis writing guide of the Graduate School of Natural and Applied Sciences, Firat University. I also declare that all information in it is correct, that I acted according to scientific ethics in producing and presenting the findings, cited all the references I used, express all institutions or organizations or persons who supported the thesis financially. I have never used the data and information I provide here in order to get a degree in any way.

25 May 2021

Azad Ibrahim HAJI

PREFACE

Heat treatment of shape memory alloy is an effective parameter to monitor characteristics of the alloys.

First and foremost, praises and thanks to God, the Almighty, for His showers of blessings throughout this thesis work to complete this thesis successfully. I would like to express my deep and sincere gratitude to my thesis Supervisor: Prof. Dr. Cengiz TATAR. I am extremely grateful for what he has offered me. I would also like to thank him for his friendship, empathy, and a great sense of humor.

I am extending my heartfelt thanks to my wife and my family for their acceptance and patience during the discussion. I am extremely grateful to my parents for their love, prayers, caring and sacrifices for educating and preparing me for my future. I am very much thankful to my wife and my daughters for their love, understanding, I would like to say thanks to my friends and thesis colleagues, Ibrahim Nazem Qader.

This thesis was supported by the project number **FF.19.01** by Firat University Scientific Research Projects Coordination Unit (FÜBAP). The studies were carried out with the permission of the Ethics Committee ... / .... / 20 ... and numbered .....

Azad Ibrahim HAJI
ELAZIG, 2021

TABLE OF CONTENTS

Page

ABSTRACT

Investigation of Microstructure and Thermodynamic Properties of NiTiCu Shape Memory Alloy Aged at Different Temperatures

Azad Ibrahim HAJI

Master's Thesis

FIRAT UNIVERSITY
Graduate School of Natural and Applied Sciences

Department of Physics

May 2021, Page: xi + 43

NiTiCu shape memory alloys are one of the mechanical heat-treatable alloys. Heat treatment has been performed to investigate the mechanical, microstructure and thermodynamic improvements in high copper-content NiTiCu alloys. In this study, Metal powders ternary NiTiCu alloys with ninety-nine percent purity were mixed. Then, the metal powders were pressed to make pellets with a 10 MPa pressure. They were produced by an arc-melting system under the argon atmosphere to obtain $Ni_{30}Ti_{50}Cu_{20}$ mole % alloy. After that, pieces of both alloys were cut and the heat treatment process has been applied at1073, 1123, 1173, and 1223K for a single hour. After the aging process, the quenching operations were performed inside ice-salted water. The differential scanning calorimetry (DSC) measurements were performed for the heat-treated specimens with heating/cooling speed rate of (10, 15, 20 and 25K/min). For investigation of microstructure, mechanical and thermodynamic properties of the heat-treated alloys, some devices were used, including DSC, SEM-EDS, Metallurgical microscope, and Vickers microhardness. Besides some mathematical calculations, such as activation energy, entropy, Gibbs free energy, and elastic energy, were performed for the forward and/or reverse-phase transformation process. Three different methods were used to calculate activation energy, whereby, the results showed nearly the same values for all cases. For the chosen range of measurements, the DSC curves showed a single phase transformation between austenite (B2) phase and martensite (B19) phase. The calculated thermodynamic parameters were affected by the heat treatment such that the alloy with 1223K aging temperature showed a maximum value compared to the other counterparts. Also increasing the temperature of aging caused to increase in the crystallite size of the alloy.

Keywords: Low Temperature Shape Memory Alloy, Phase transformations, Heat treatment, Microhardness

ÖZET

Farkli Sicakliklarda Yaşlandirilan NiTiCu Şekil Hafizali Alaşimin Mikro Yapisinin Ve Termodinamik Özelliklerinin İncelenmesi

Azad Ibrahim HAJI

Yüksek Lisans Tezi

FIRAT ÜNİVERSİTESİ
Fen Bilimleri Enstitüsü

Fizik Anabilim Dalı

Mayıs 2021, Sayfa: xi + 43

NiTiCu şekil hafızalı alaşımlar, mekanik ısıyla işlenebilir alaşımlardan biridir. Yüksek bakır içerikli NiTiCu alaşımlardaki mekanik, mikro yapı ve termodinamik gelişmeleri incelemek için ısıl işlem yapılmıştır. Bu çalışmada, yüzde doksan dokuz saflığa sahip metal tozları üçlü NiTiCu alaşımları karıştırıldı. Daha sonra metal tozları, topaklar yapmak amacıyla 10 MPa'lık bir basınçla baskılandı. $Ni_{30}Ti_{50}Cu_{20}$ wt % alaşımı elde etmek için argon atmosferi altında bir arkla eritme sistemi ile üretildiler. Bundan sonra, her iki alaşımın parçaları kesildi ve ısıl işlem süreci, bir saat boyunca 1073, 1123, 1173 ve 1223K'da uygulandı. Yaşlandırma sürecinden sonra, buz tuzlu su içinde söndürme işlemleri gerçekleştirildi. Isıtma/soğutma hızı oranı (10, 15, 20 ve 25K / dak) olan ısıl işlem görmüş numuneler için diferansiyel tarama kalorimetresi (DSC) ölçümleri gerçekleştirilmiştir. Isıl işlem görmüş alaşımların mikro yapısının, mekanik ve termodinamik özelliklerinin incelenmesi için DSC, SEM-EDS, Metalurjik mikroskop ve Vickers mikro sertliği gibi bazı cihazlar kullanılmıştır. Ayrıca, ileri ve/veya ters faz dönüşüm işlemi için aktivasyon enerjisi, entropi, Gibbs serbest enerjisi ve elastik enerji gibi bazı matematiksel hesaplamalar yapıldı. Aktivasyon enerjisini hesaplamak için üç farklı yöntem kullanıldı ve böylece sonuçlar tüm vakalar için neredeyse aynı değerleri gösterdi. Seçilen ölçüm aralığı için DSC eğrileri, ostenit (B2) fazı ile martensit (B19) fazı arasında tek fazlı bir dönüşüm göstermiştir. Hesaplanan termodinamik parametreler, 1223K yaşlandırma sıcaklığına sahip alaşımın emsallerine kıyasla maksimum bir değer göstereceği şekilde, ısıl işlemden etkilenmiştir. Aynı zamanda yaşlandırma sıcaklığının artırılması, alaşımın kristalleşme boyutunda artışa neden olmuştur.

Anahtar Kelimeler: Düşük sıcaklık şekil hatırlamalı alaşım, Faz dönüşümleri, ısısal davranışlar, Mikrosertlik

LIST OF FIGURES

Page

LIST OF TABLES

Page

SYMBOLS AND ABBREVIATIONS

Symbols

A_s : Austenite start

A_f : Austenite finish

M_s : Martensite start

M_f : Martensite finish

B19 : orthorhombic martensite

B2 : cubic austenite

B19’ : monoclinic martensite

E_a : activation energy

β : Heating rate

R : the universal gas constant

T_p : the maximum peak temperature

PTTs : peak time temperature

dq/dt : the instantaneous heat gained

T : the absolute temperature

t : the time

Eq. : Equation

ΔH : enthalpy change

ΔH_{fr} : internal friction

ΔH_{ch} : chemical energy

ΔH_{el} : strain energy

ΔS : Entropy change

T_o : Equilibrium temperature

ΔS_{vib} : vibrational contribution

ΔS_{el} : conduction electrons

ΔS_{mag} : magnetic subsystem

ΔS_{dist} : Brillouin zone distortion

ΔS_{conf} : configuration contributions

ΔG : Gibbs free energy

ΔE_e : Elastic energy

A_f : austenite finish temperature

D : crystallite size

B : wideness at half maximum

θ : Bragg's angle

λ : Wavelength

℃ : degree Celsius

X : axis Horizontal

Y : axis vertical

σ_s : start stretch level

ε : strain

Pa : Pascal

K_α : first excited state of copper

HCl : Hydrochloric acid

mL : mili liter

s : second

h : hour

α : alpha

K : kelvin

Å : Angstroms

Abbreviations

Cu : Copper
DSC : Differential Scanning Calorimetry
EDX : Energy Dispersive X-ray spectroscopy
Ni : Nickel
SEM : Scanning Electron Microscope
SMA : Shape Memory Alloy
Ti : Titanium
EDS : Energy dispersive x-ray spectroscopy
XRD : X-Ray Diffraction

1. INTRODUCTION

Shape memory alloys (SMAs) are one class of the advanced materials that recently as a modern type of materials have been used in many applications around the world. The unique capabilities that they have, make them be studied by researchers to improve their mechanical, magnetic, electrical, thermal properties Shape memory effect (SME) and pseudoelasticity are two differences that these kinds of alloys can show compared to the other known materials. Till now, many families have been found, whereas, nearly equiatomic NiTi SMAs obtained a wide attraction compared to the other families. They are used in various fields such as medicine [1], robotics [2], and SMA-based actuators [3]. It is proved that the characteristics of SMAs are affected by many factors, such as compositional rate [4-8], type of constituent chemical elements [9], manufacturing techniques [10], surface treatment [11], and heat treatment effects [12-14].

One of the wide studied shape memory alloys is NiTiCu SMAs. NiTiCu SMAs depend on heat treatment and thermomechanical cycling [15]. For example, Tatar et al. [16] found that the crystallite size growth with increasing copper-content in NiTiCu SMA. Fabregat-Sanjuan and colleagues [17] investigated the effect of aging on the internal friction and storage modulus of Ni-Ti-Cu SMA. They reported that the produced dislocation, formed by hold work, was disregarded by the heat treatment, and therefore, it influenced on the tan δ and storage modulus. In another work, Shi et al. reported that the internal friction reduced with increasing the aging temperature [18]. The dislocations can produce internal stress in SMAs, and thus they make an obstacle for austenite phase transformation. Therefore, this issue can be solved by utilizing aging in high temperatures [19]. There are not heat treatment investigations on the microstructural, mechanical and other thermal behavior of high Cu-content NiTiCu SMAs.

In this master thesis, we have tried to investigate the influence of the temperature dependence aging parameter on a high Cu-content NiTiCu SMA. We have produced NiTiCu alloy by using the arc-melting method and four different pieces of the alloy have aged at 1073, 1123, 1173, and 1223 K for one hour. Some important measurements have been carried such as differential scanning calorimetry, x-ray diffraction, Vickers microhardness, optical microscope, scanning electron microscope, and energy dispersive x-ray spectroscopy. The obtained results showed information about thermal, mechanical and microstructural properties of the as-aged NiTiCu SMAs. Furthermore, some related calculations have been performed to investigate the SMAs characteristics, more deeply. In chapter two, we have briefly defined shape memory alloys and their general characteristic. In chapter three, the materials and different measurements and techniques have been explained. In chapter four, we deeply analyzed the results and they have been compared with literature. Finally, in chapter five we summarized the outcomes of this study.

2. CHARACTERISTICS AND TYPES OF NiTi-BASED SMAs

It is worth to define shape memory alloys (SMAs) and the characteristics that make them different from the other kinds of alloys. In addition, some of SMAs have some other common properties that are more applicable compared with the other alloys, e.g., the equiatomic NiTi alloy, in its austenite phase, is as stiff as stainless steel.

2.1. Definition

Shape memories can be defined such that they can recover their unique shape from an imperative and plastic twisting when an extraordinary stimulant is applied. Also, an alloy has unique properties that exist in the parent constituents. A metallic alloy is a combination of two or more different chemical elements. Generally, the constituents do not make a chemical bond, but they dissolved into each other or in some specific areas making their phases. The rate of dissolving and microstructures can give different properties to the alloy. In the solid phase, a shape memory alloy has two different atomic orders, which are known as austenite (in higher temperature) and martensite (in lower temperature). Figure 2.1 shows the mechanism that the crystal structure of a SMA is transformed from one to the other. The austenite phase has a more similarity and is stable at high temperatures. However, the martensite phase has a different crystal structure, which is a non-cubic crystal, e.g., monoclinic (B19’ in equiatomic NiTi alloy) or orthorhombic (B19 in high copper-content NiTiCu).

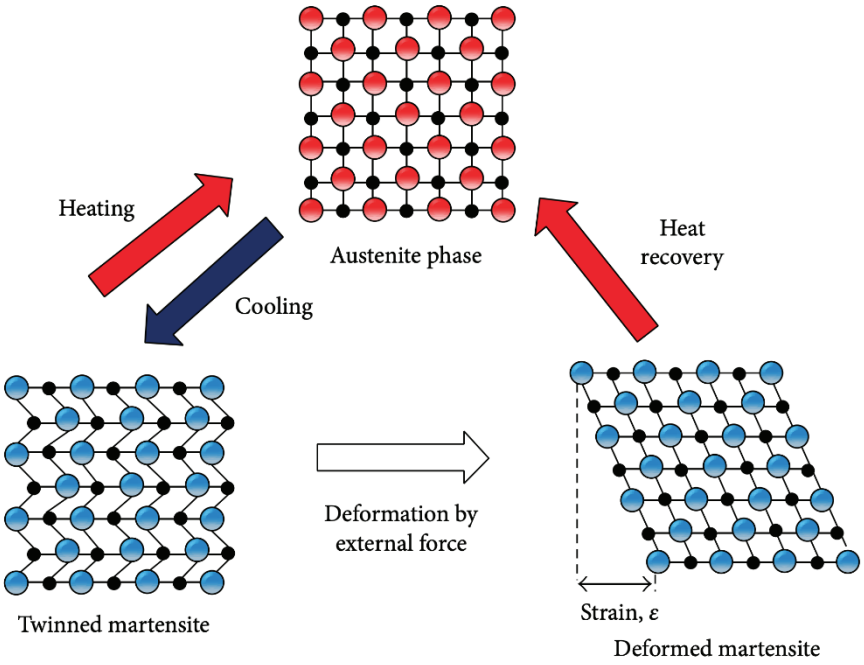

Figure 2.1. Different phases of an SMA [20]

2.2. Crystal Structures and Micro-Structure

A crystal is a net with an ordered arrangement that consists of atoms, ion, or molecule [21]. In the world around us, all solid materials are made of either crystalline or amorphous that has no ordered arrangement. In nature, most metallic materials exist in crystalline type. The type of crystal gives different physical properties to the material. For example, graphite and diamond are two different materials that fundamentally consist of carbon, however, the differences in atomic arrangement make these differences. Although materials mostly have a specific crystal structure, alloys may have different crystal structures, which depend on the composition and/or temperature. In shape memory alloys, the transformation between two different crystal structures happens whenever the temperature is changed.

Figure 2.2 shows a NiTi alloy with two different crystal structures. In lower temperatures, the NiTi shape memory alloy has a zigzag (or twined structure), which is known as a monoclinic crystal structure. In some particular cases, the atoms in NiTi can be ordered as an orthorhombic martensite (low temperature) phase. On the other hand, in the nearly equiatomic NiTi shape memory alloy, the atom of nickel and titanium creates a superlattice with cubic lattice, which has higher similarity compared with the lower temperature phase. The Austenite phase sometimes is called the parent phase because it has a crystal structure like the most metallic materials. The existing differences are important for shape-memory materials. In addition, it is reported that lots of metals have frequent crystal structures at the same composition, nonetheless, most metals do not display shape-memory effect (SME). This is a particular feature that lets the shape-memory alloys to return to their first shape after increasing temperature by the heating process.

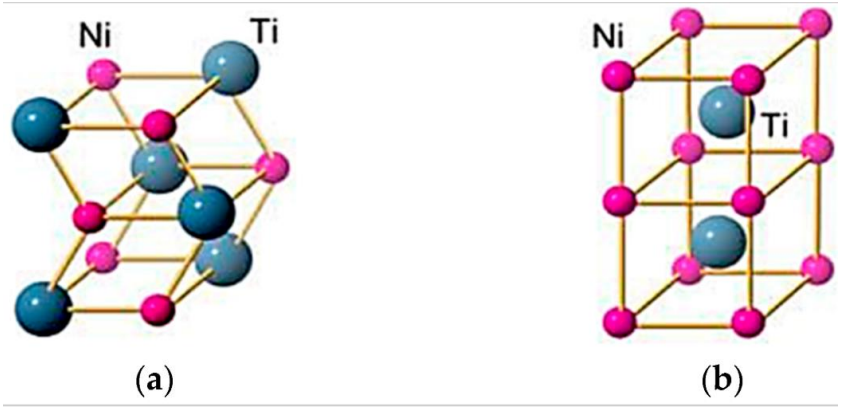

Figure 2.2. The crystal structure for a NiTi alloy with (**a**) martensite-B19′, and (**b**) austenite-B2 phases [22]

The number of crystal structures consists of 14 types, but far from these crystal structures, there are countless numbers of microstructures the can be seen with aid of an optical microscope or scanning electron microscope. Since the can be observed in the microscope range, so they are

known as microstructures, i.e., they are very small, which defined as the structures revealed by an optical microscope above 25× magnification [23]. It is proved that the microstructure of a material such as metals, polymers, ceramics, and composites can directly affect physical characteristics like strength, toughness, ductility, hardness, and corrosion resistance. Besides, when the size of the microstructure is in the nano-scale and could not be detected by the optical microscope is called nano-structure. Even smaller than nano-structure, the individual atoms are arranged, which is defined before as crystal structure.

Figure 2.2a reveals a NiTi shape memory alloy with martensite (twinned monoclinic B19′ structure). In the austenitic phase, NiTi SMA has a highly symmetric, represented as B2 structure Figure 2.2b. martensite has a needle-like herringbone shape. Also, the austenite NiTi alloy is harder and stiffer than martensite-NiTi alloy [22].

Figure 2.3 showed how annealing influence on the microstructure of a NiTi alloy. Losertová et al. showed that annealing in high temperature changes the microstructure of NiTi alloy and hence the hardness of the alloy was affected [24].

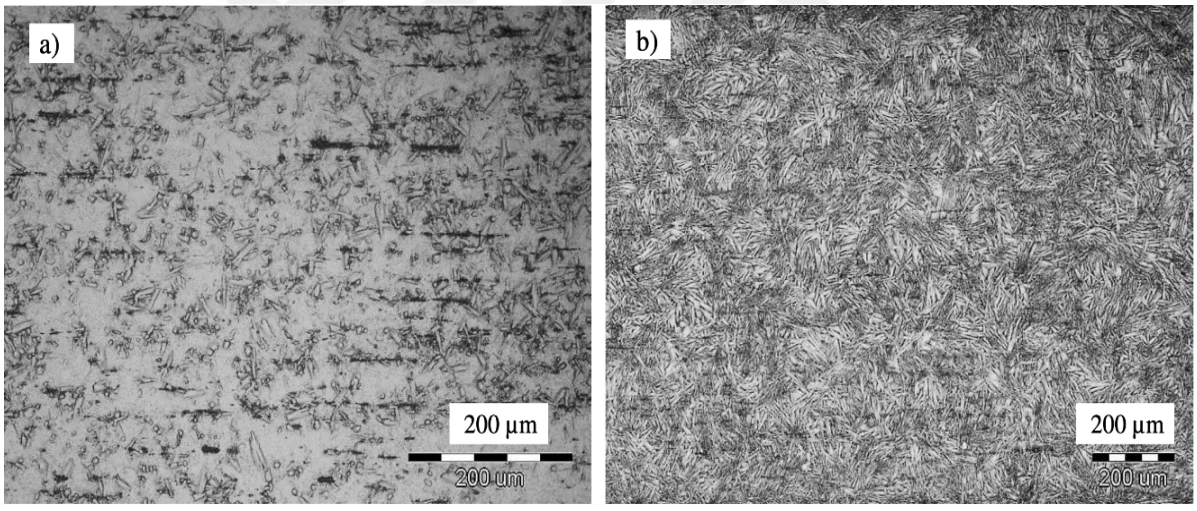

Figure 2.3. Microstructure of a NiTi alloy annealed at 873 K for 1 h, water quenched and aged for 0.5 h a) at 563 K and b) at 623 K [24]

2.3. Phase Diagram

A phase diagram is a graph that is usually used for showing the different phases of material with various environmental conditions, such as temperature, pressure, and composition. The diagram can show the boundaries between solid, liquid, and gaseous phases of material with a single substance or a mixture of substances. In alloys, particularly in shape memory alloys, two variables are taken into account and the other keeps constant. Temperature and composition (amount of constituents) are two significant parameters that represent y and x-axes of the diagrams. Figure 2.4 illustrates the phase diagram of Ni-Ti alloy with different compositions and in a

particular range of temperatures. Various phases consist of a single or a combination of phases. In a low concentration or high concentration of the diagram, the phases make of s single atom with a solution of the impurities. By increasing the amount of doping, a new phase based on different structures obtained, which also differs from changing temperature. In the nearly equiatomic concentration, the NiTi alloy has a V-shape that separated by a transformation temperature (horizontal line / 630 ℃). The bottom of the V-shape is called eutectoid, which is a crucial point that makes distinguish between a shape memory material from ordinary material. In shape memory alloys, the upper phase is called austenite and the phase under the transformation temperature is called the martensite phase.

Heat Treatments is one of the important factures to improve the physical properties of NiTi alloy that can be performed with the aid of the phase diagram [25].

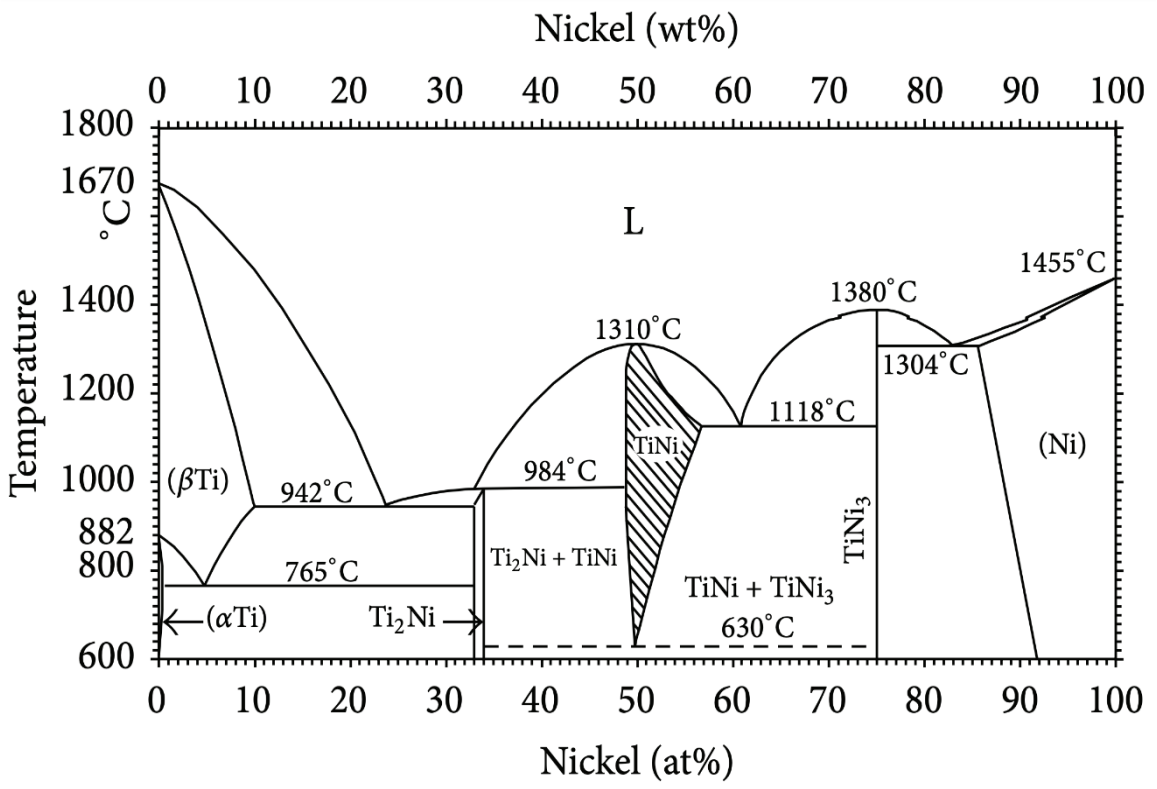

Figure 2.4. The Ni-Ti phase diagram [25]

2.4. Special properties

SMAs are two bases consist of copper and nickel from engineering materials. This composition can be manufactured to any shape and size.

The resistivity of shape memory alloys is lower than that of conventional steels, but plastic or aluminum have lower strength than the compositions. NiTi its yield stress is up to 500 MPa. If it's the same metal it will cost more and the processing requirements are difficult and expensive to

implement SMAs in the design. This material in SMAs is used in the workplace and may be neglect the properties of shape memory effect and super elastic. Its application is known to work.

Like on this one of the benefits of SMAs is at a higher level of return than a plastic strain. The highest return pressure of SMAs is maintained without damage up to 8% and some materials compare the highest pressure level of return for conventional steel up to 5% [26].

2.4.1. Superelasticity

One of the known properties that all materials can show is the elasticity that can be monitored using the stress-strain test. There is a linear relationship between exerted stress (either compression or tensile) and the obtained strain. An extraordinary force can make a slip in the atomic arrangement, and hence, a permanent deflection occurs. On the other hand, shape-memory materials can transfer the extra force into a new rearrangement of the atoms, which is called the phase transformation process. This extra-ordinary property is called pseudoelasticity or superelasticity. After the stress is removed the restoring force returns the shape to its pre-determined morph, while some energy consumed during these transformations causes a hysteresis.

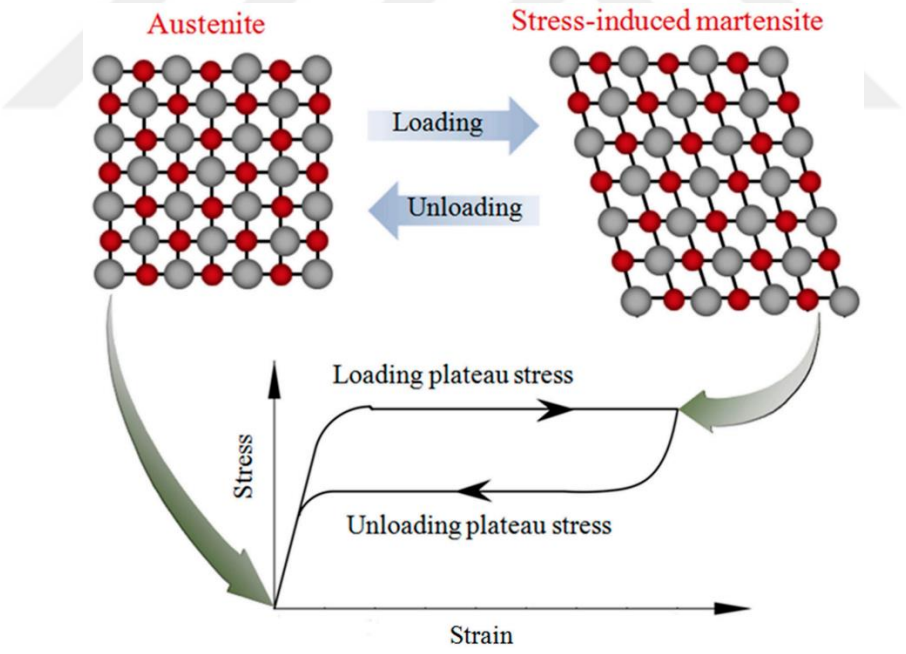

Figure 2.5: Psudoelasticity or superelasticity [27]

Figure 2.5 shows the superelasticity of a shape memory alloy, where the cubic crystal structure under an external load and above austenite finish temperature can transfer to the metastable martensite phase, then twinned martensite changed detained martensite by increasing the load. After that, when the load is removed, the single variant detwinned martensite phase

transferred starts to transform into the austenite phase. All process is shown in a stress-strain diagram which includes a straight line (elasticity), plague (transformation from austenite to martensite phase and vice versa) and returns to the original point [28].

2.4.2. Shape Memory Effect

Shape memory effect (SME) is one of the changes in the SMA by temperature changes, and it passes in several stages, the first stage SMA by cooling converts to the twinned martensitic stage, the second stage the twinned martensitic by a pressure method converts to the deformation martensitic, the last deformation martensitic by the heating transformed into The original place (the parent austenitic stage) as seen in Figure 2.6. In this diagram showing the two axes, the axis (X) is stress on the material and the axis (Y) is pressure on the material.

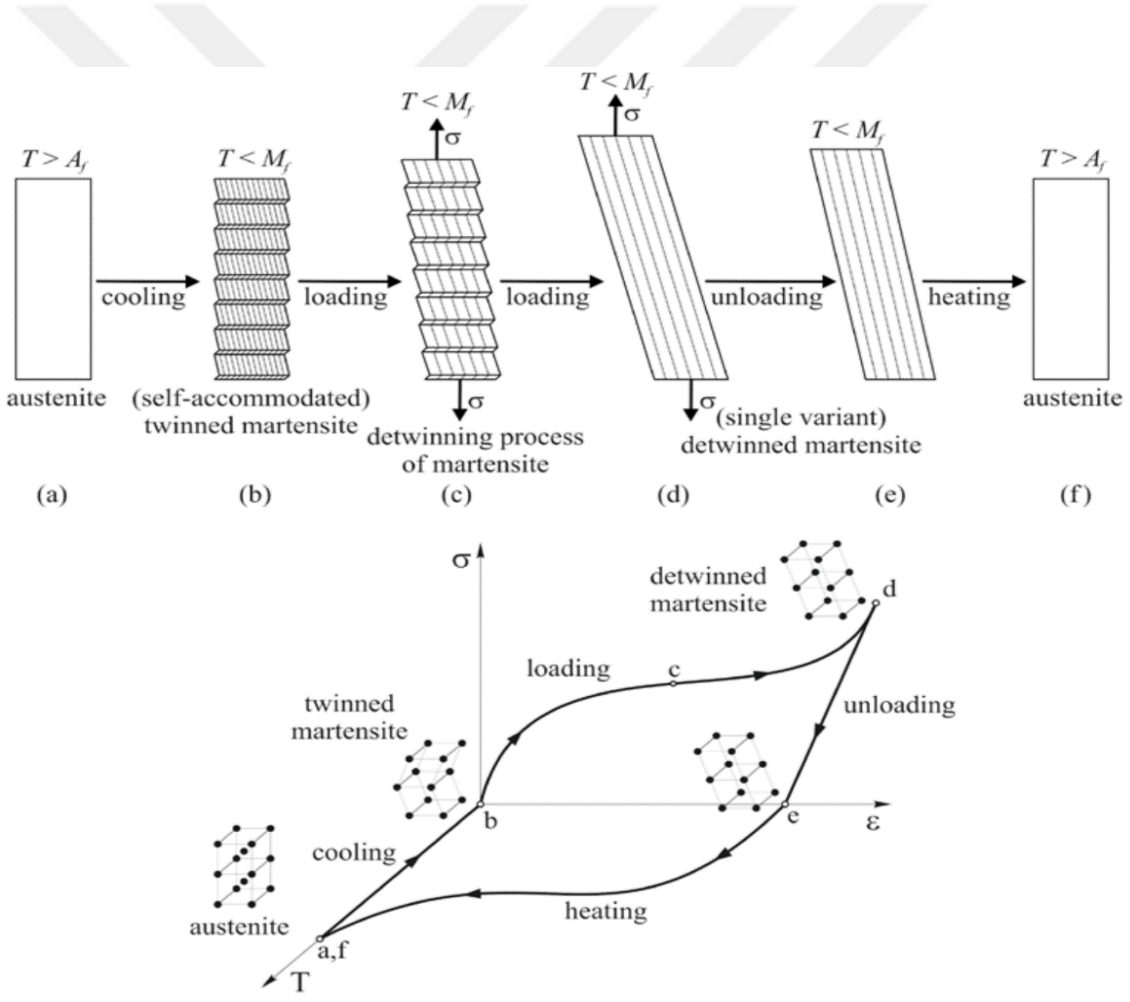

Figure 2.6. Schematic representation of the shape memory effect [27, 29]

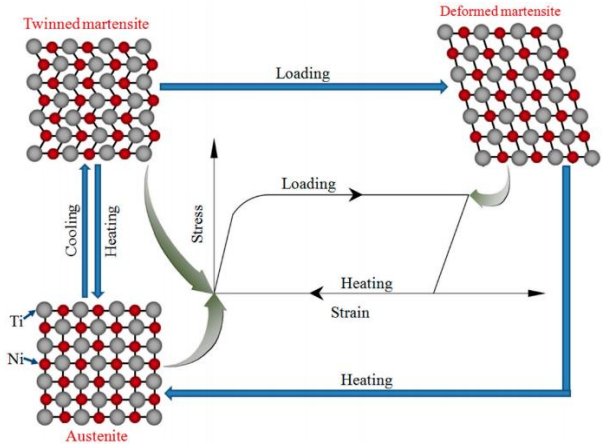

Figure 2.6. Schematic representation of the shape memory effect (continue)

The Point (*A*) in Figure 2.6 is in the original stage, and in this cooling stage, there is no austenite stress at variable temperatures versus the start of martensite and the end of martensite. Then the point (B) in this organization of twinned martensite. The twinned martensite is stretch at any time the change of the start stretche level (σ_s), the beginning process of and there start way, the same time the differences martensitic is the good way development and another calculation the end differences martensitic is decrease favorable. In this case, the martensite taking the stretch permanent plastic higher than the pressure level act of changing the direction of a changed distance, σf, the last tableland making that's characterized in the σ-ε graph in Figure 2.6. In a flexible shape from point C to D, the fabric is discharged, held the detwinned martensitic state in point C to D. the pressure is hiding when the high hot, any time the temperature gets to the as beginning different the change (at E) and the finished in the temperatures A_f (point F) that point it has the parent austenitic stage. Any time detwinning starting the permanent plastic strain is not showed, the SMA is a return to the first shape looked at this point A. the changing strain (ε_t) It is a reason that is changing from detwinned martensite to austenite SME, which is a process change that heats this material from the detwinned martensite it is beginning and at the end to returning to its original place, by the united mechanical load [30].

2.5. Heat treatment

As has been clarified, the temperature and heat heating/cooling process are straightly affected on microstructures and hence, the other thermal and mechanical properties of shape memory alloys are affected. Losertová et al. investigated the effect of aging at different temperatures after annealing process followed by quenching into the ice-brined medium (Figure 2.7). They found the annealing process was more effective on Vickers microhardness compared to the aging process. Marattukalam et al. found that annealing equiatomic-NiTi alloy at 500 and 1000 °C led to an

increase in the crystallite size of the alloy [31]. Liu et al. [32] reported that heat treatment can affect the damping characteristic of NiTi shape memory alloy. Bujoreanu et al. showed the influence of heat treatment on the tensile pseudoelastic response and other thermodynamical parameters of a Ni-rich NiTi SMA [33]. Figure 4.8 reveals the effect of annealing on the R-phase, which was produced after the annealing process.

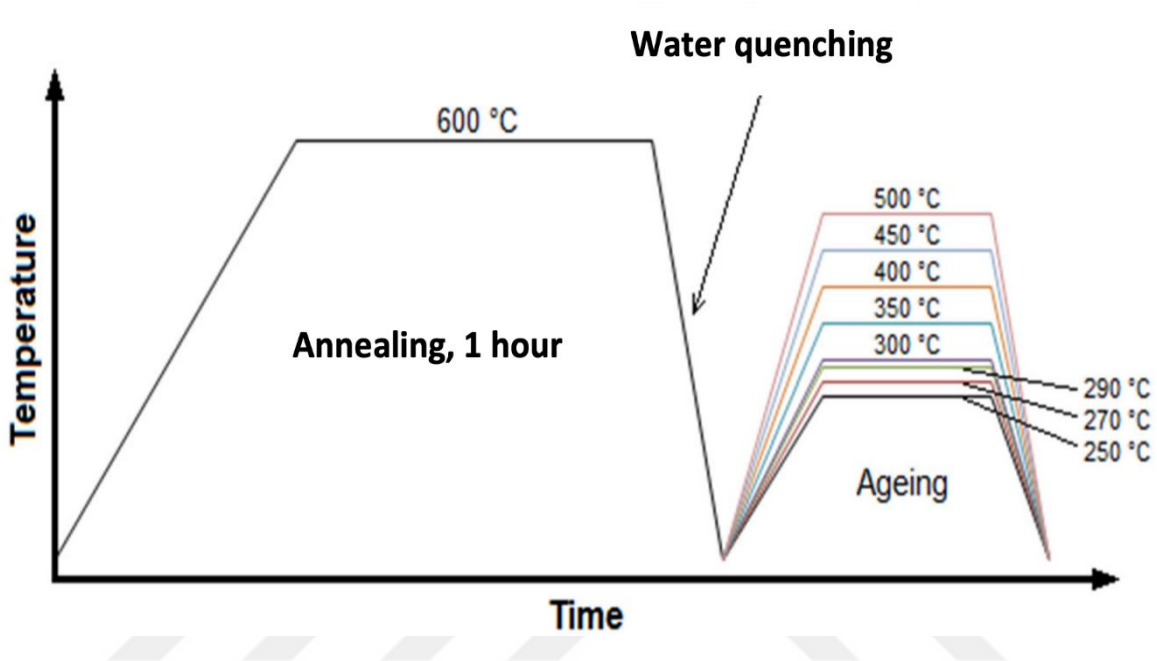

Figure 2.7. Schematic of heat treatment of NiTi samples [24]

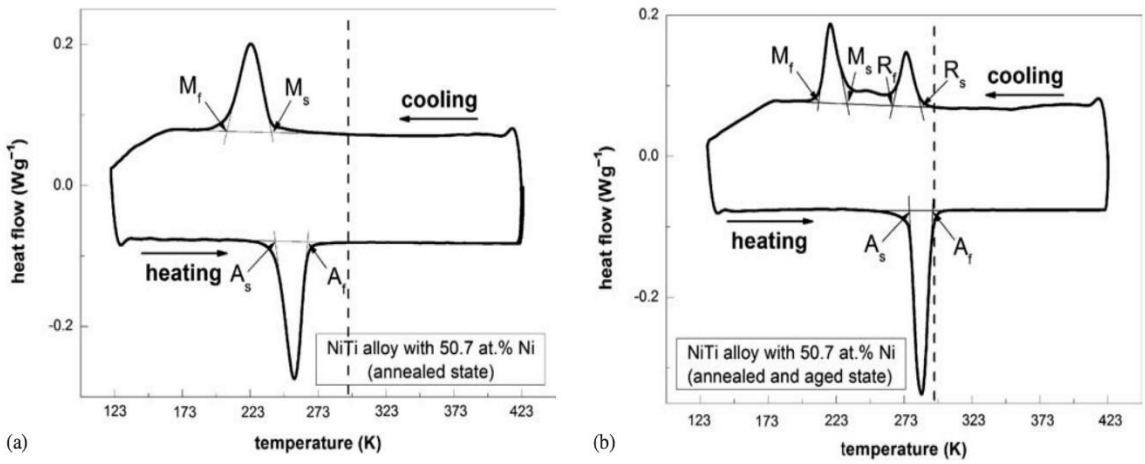

Figure 2.8. DSC charts for n $Ni_{50.7}Ti_{49.3}$ SMA in an (a) annealed state and (b) annealed and aged state [33]

3. MATERIALS AND EXPERIMENTAL PROCEDURE

To write a report on a topic, we need deep thinking to start work. We need to arrange and divide the material in order to reach the right path, as well as working with other people leads to make easy things towards progress and more.

We need reality results, to write the report. Sometimes the methods do not lead to the correct results. In the beginning, the parts of the material and its methods have an important role in preparing the correct report, and every correct report needs correct thinking.

It is also a very important count for anyone who can benefit from it and refer to it wherever he is, and from a scientific point of view the repeating of results is very important. In general, in terms of material and methods, errors occur in laboratory reports, and a scientific decision must be taken at a high level, and sometimes mistakes are made in the last part of the report [34]**.** Materials

The materials used for this study consist of three different chemical elements, including the 30-mole percentage of nickel (30 at. % Ni), 50-mole percentage of titanium (50 at. % Ti), and 20-mole percentage of copper (20 at. % Cu). The constituents have chosen from high pure powders.

3.1. Manufacturing

The powders were poured into a mixture to be mixed. After, the powders well mixed, the mixture was subjected to nearly 10 MPa to form some compacted cylinders. The pellets were put in the special groves of an arc-melting device (Figure 3.1). The chamber of the device was vacuumed to 10^{-5} Pa and then it filled with argon gas, which is an inert gas. The inert gas was used as an atmosphere because it avoids oxidation in high temperature and it needs as a medium path between the arc and the sample. The sample was heated up until it melts then it cooled down to room temperature in the device's chamber. Before the chamber was opened, it again vacuumed to expel the dangerous obtained gas during the melting process,

Figure 3.1. The arc-melter device with an atmosphere control chamber. It has two pumps and a high power supply

3.2. Cutting Process

The obtained ingot (NiTiCu alloy) was cut using an electric mini grinder drill (Figure 3.2) model DREMEL. For each measurement, a sufficient piece was cut, e.g., four samples for DSC and four samples for SEM. The size of samples for different measurements had to be chosen differently. For example, the SEM test needs a convenient surface, while for DSC the size and geometry are not important but the sample should fit the crucible.

Figure 3.2. Electric Mini Grinder/Micro Drill (DREMEL)

3.3. Heat Treatment

After preparing some sufficient samples from the ingot, the specimens were put inside a furnace. Figure 3.3 shows the furnace that was utilized for the aging process. In the beginning, the furnace was set for a specific temperature. After the temperature reaches the determined temperature, the specimen was put in the furnace. There were four different temperature were determined, including 1073K (800℃), 1123K, (850℃), 1173K (900℃), and 1223K (950℃). The samples were labeled according to their aging temperature, such that C1, C2, C3, and C4 were chosen for 1073K, 1123K 1173K, and 1223K, respectively.

After one hour of aging, the samples were quenched (fast cooling) into ice-brined (≅ 0℃). This cooling process, lets samples have a diffusionless transformation from the high-temperature phase (austenite) into the low-temperature phase (martensite). Then the samples were dried from the water using a hairdryer to avoid oxidation happened on the surfaces of the alloys. The samples then were ready for characterizations.

Figure 3.3. Furnace for aging alloys (PROTHERM)

3.4. Characterization Processes

In this study, many characterizations were carried out. In the following sub-sections, the techniques and instruments used for characterization of the as-aged alloys have been explained with corresponding photos.

3.4.1. Differential Scanning Calorimetry (DSC)

Differential scanning calorimetry (DSC) is a device consists of two crucibles, one of which is a container intended for the tested sample and the other is left empty, which is the reference vessel. The two crucibles are placed in a chamber that is usually heated with a certain rate, such as 10 degrees Celsius per minute. Under each crucible, there is a thermocouple connected to a computer to record the temperature change during the heating and cooling process at a constant rate. The computer software can subtract the sample's temperature from the reference. The recorded data were plotted with a specific software program. Also, the data was extracted for more analyzing and founding some thermodynamics parameters. This measurement is one of the crucial measurements in this type of study. Some of those thermodynamics' parameters are phase transformation temperatures that can be found by using the intercept of two tangential lines from starting or finishing the transformation process.

Figure 3.4. Differential Scanning Calorimetry (Perkin Elmer Sapphire)

The DSC used in this study was (Perkin Elmer Sapphire (Figure 3.4). The DSC was run with 10, 15, 20, and 25 K/min to found the activation energy. The chosen range was between 223 K and 400 K. The nitrogen was used during both heating and cooling processes.

3.4.2. X-Ray Diffraction (XRD)

Figure 3.5 shows the x-ray diffraction, model (RIGAKU D / MAX-B GEIGERFLEX). The device was used for the crystal structure of the alloy and to monitor the influences of aging temperature on the investigated alloys. The measurement was conducted from 30 to 80 degrees. Also, it runs at room temperature, in which the samples were in the martensite phase. The samples were well prepared and their surface had no dust or oxide layer, thus the results only showed the phases made of the existing constituents of the alloys. The x-ray that used was obtained from the transition of an electron from the first excited state of copper, known as K_{α}. The wavelength of the x-ray was 1.5 nm, which was sufficient for the x-ray diffraction pattern.

The x-ray diffraction pattern is the intensity of the signal for various angles of diffraction at their respective two theta positions, and the two theta positions correspond to the certain spacing between the crystals or atoms in the samples, determined by the angle of diffraction from the incident x-ray beam sent into the sample. Therefore, the intensity of the peaks is related to the number of molecules in that phase or with that spacing. The greater the intensity of the peak, the greater the number of crystals or molecules with that distinct spacing. In addition, the width of the peaks is inversely proportional to the crystal size. A thinner peak corresponds to a smaller crystal. A broader peak means that there may be a larger crystal, defect in the crystalline structure, or that the sample might be amorphous in nature, a solid lacking perfect crystallinity. Then, for smaller samples, the patterns determined using XRD analysis can be used to determine a sample's composition. There is a large database of elements, compounds, and minerals that contain the diffraction patterns for elements, compounds, and minerals. The pattern for an unknown compound was compared to the literature and experimentally determined values verify the identity of an element, matching the location, width, and relative heights of the diffraction patterns

Figure 3.5. The X-Ray Diffraction device (RIGAKU D / MAX-B GEIGERFLEX)

3.4.3. Microstructure Analysis

The microstructure of the aged alloys was investigated using a metallurgical microscope (Figure 3.6) PRIOR Model -N334 Incident Light Metallurgical Trinocular Microscope. The samples were cleaned to observe microstructures as well as possible. The surface of the as-aged alloys was grinned and etched.

Figure 3.6. PRIOR Model -N334 Incident Light Metallurgical Trinocular Microscope

Figure 3.7. Scanning electron microscope and energy dispersive x-ray spectroscopy

The second analysis was carried out using a scanning electron microscope (SEM). Figure 3.7 reveals the SEM device that was used in this study. Similar to an optical microscope, to obtain a clear SEM image, the samples were grinned and smoothed then etched with 20 mL HCl–96 mL methanol–5 gr Fe_3Cl–H_2O solution. Besides, the device was used for the chemical composition of

some areas. Energy dispersive x-ray spectroscopy (EDS) can clearly show the composition of metallic alloys.

3.5. Vickers microhardness

The last measurement was Vickers microhardness to found a mechanical property of the alloys. The tests were performed by (Emco Test DuraScan) with a load of 50 g for 10 s. Each test was carried out for matrix and second phase in three different positions. The average value and standard deviation were used to analyze and make a comparison between the aged alloys. Figure 3.8 shows a Vickers microhardness that was used to test the hardness of the alloys.

Figure 3.8. Vickers microhardness (Emco Test DuraScan)

4. RESULTS AND DISCUSSIONS

The DSC results for the as-aged Ni-Ti-Cu alloys is given in Figur. The time of aging is unique for all samples and the samples have been tested in the same environmental conditions. The heating process represents the reverse process, where an endothermic reaction occurred due to phase transformation from the martensite phase to the austenite phase. On the other hand, the cooling process represents the forward process, in which an exothermic process has happened from austenite to the martensite phase. In either forward or reverse phase transformation, only a single peak or trough can be seen that indicates there is no noticeable intermediate phase created between austenite and martensite phase transformation. It is reported that a precipitated compound that can produce a double peak or trough during phase transformation Ti_3Ni_4 phase that created in the annealed NiTi SMAs with high Ni content [35, 36]. For NiTiCu shape memory alloys, it has been found that in high copper content, the alloy can show phase transformation between orthorhombic B19 and cubic B2 phases. B2 is the higher temperature phase and B19 is the lower temperature phase. Both of them could be detected using a Perkin Elmer DSC device for the temperature range of 223 K (-50 ℃) to 673 K (400 ℃). In the lower temperature, it is reported that another phase transformation can between orthorhombic B19 and monoclinic B19′ phases [37, 38].

There were four different heating rates were used for measuring heat flow as a function of temperature. The DSC results were used to find activation energy. Activation energy is a quantity of energy need for a chemical reaction to proceed [39]. It was discovered in 1880 by Swedish scientist Svante Arrhenius [40]. In this study we used three different existing models to calculate activation energy, including Kissinger equation [41], Ozawa equation [42], and Takhor equation [43, 44], which respectively are as follows:

$$\frac{d\left(\ln(\alpha/T_p^2)\right)}{d\left(1/T_p\right)} = -\frac{E}{R} \tag{4.1}$$

$$\Delta E \cong -2.19R - \frac{d\log\beta}{d\,(1/T_p)} \tag{4.2}$$

$$\frac{d(\ln(\alpha))}{d\left(1/T_p\right)} = -\frac{E}{R} \tag{4.3}$$

where E, β, and R represent activation energy, heating rate, and the universal gas constant (R = 8314 J mol^{-1}), respectively; T_p is the maximum peak temperature (austenite or martensite peak). We substitute the value of austenite peak temperature in Eqs. (4.1-4.3) to find E values for the as-aged alloys. Figura-c reveals the plots for each model. The fitting line was obtained by the Origin Lab program (version 2018), also for each linear line, a slope was obtained. The slope values were used in Eqs. (4.1-4.3) to find activation energy.

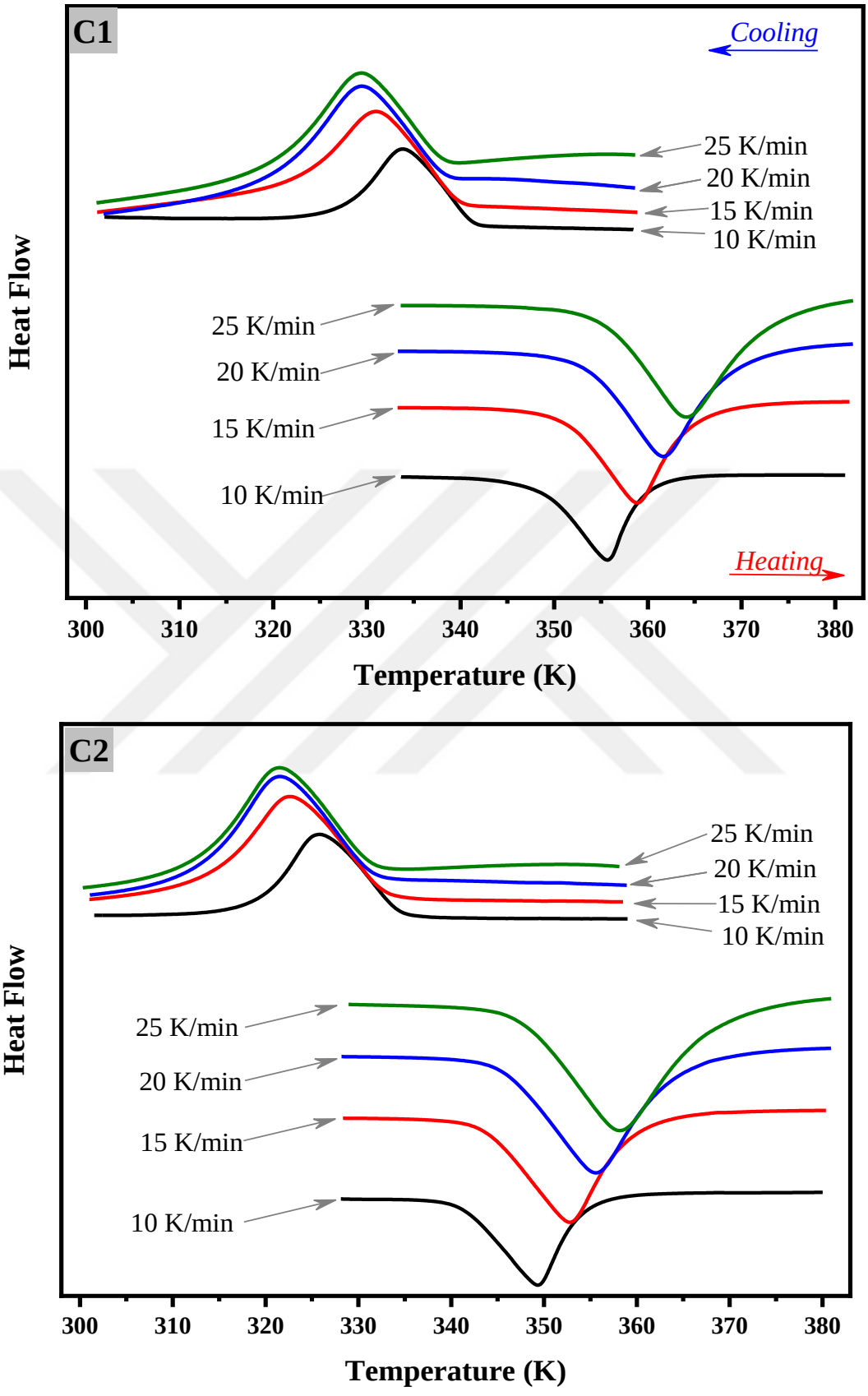

Figure 4.1. The DSC results of the aged NiTiCu SMAs for different heating rates

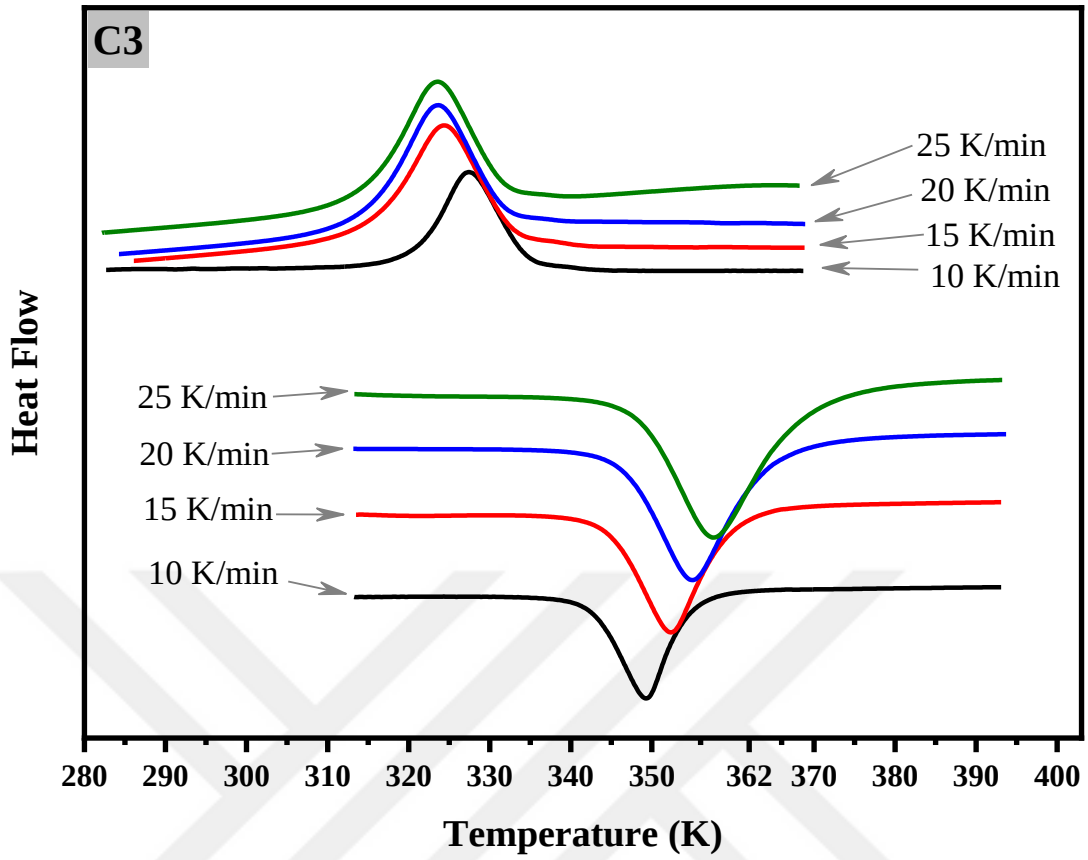

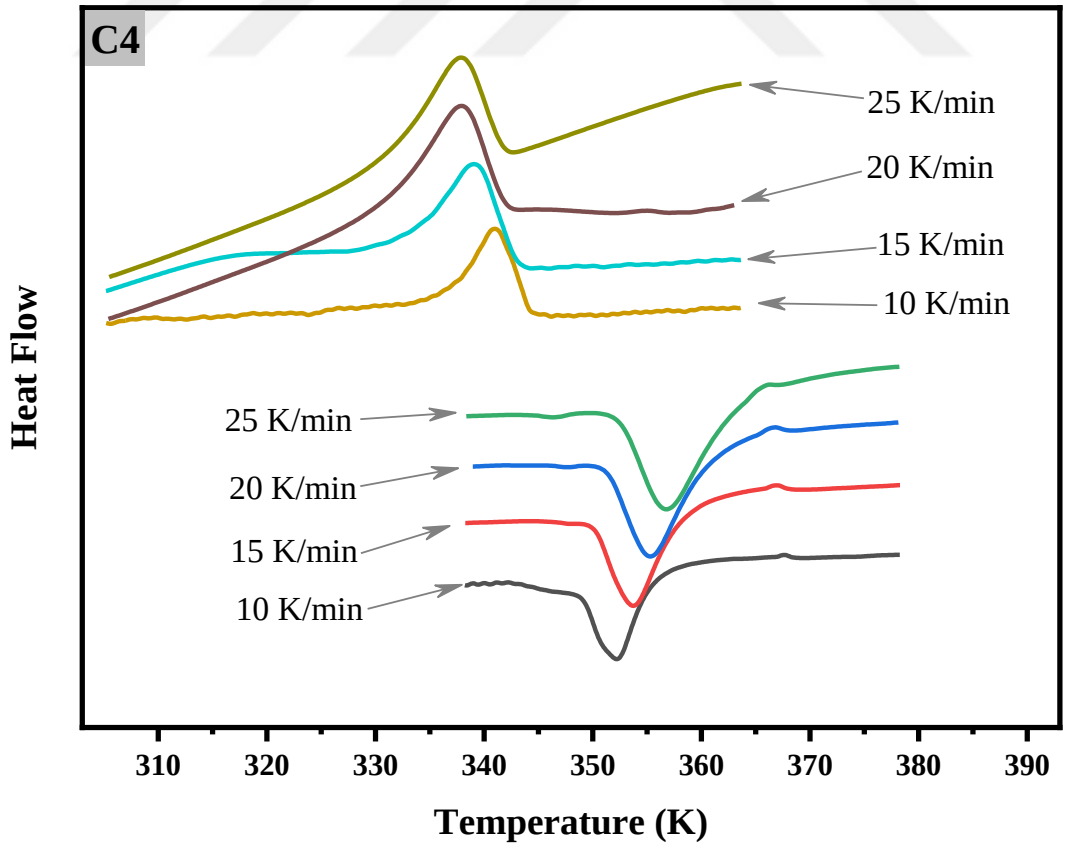

Figure 4.1. The DSC results of the aged NiTiCu SMAs for different heating rates (continue)

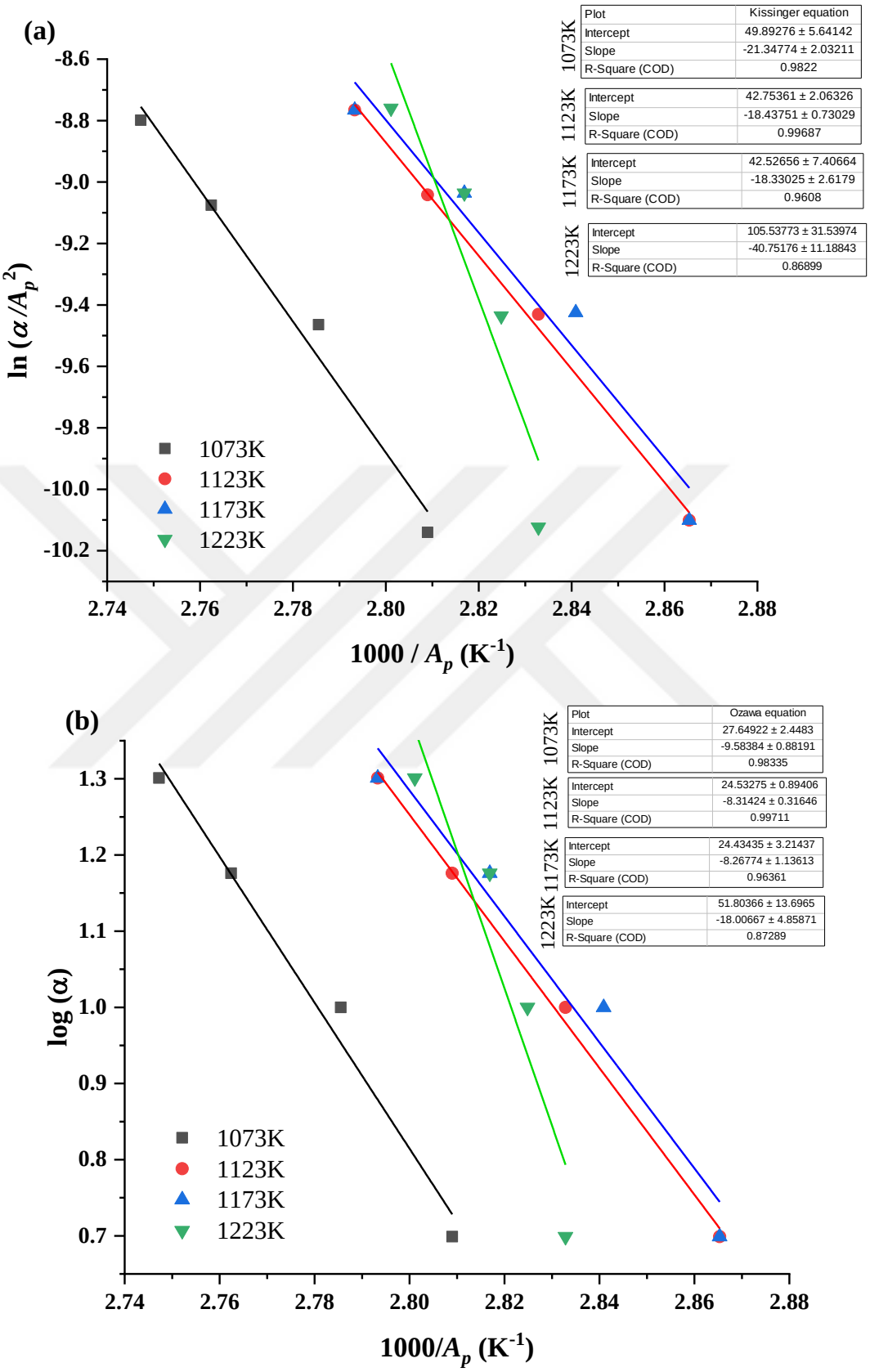

Figure 4.2. Activation energy calculated by (a) Kissinger, (b) Ozawa, and (c) Takhor equations. (d) A comparison between Activation energy as a function of aging temperature

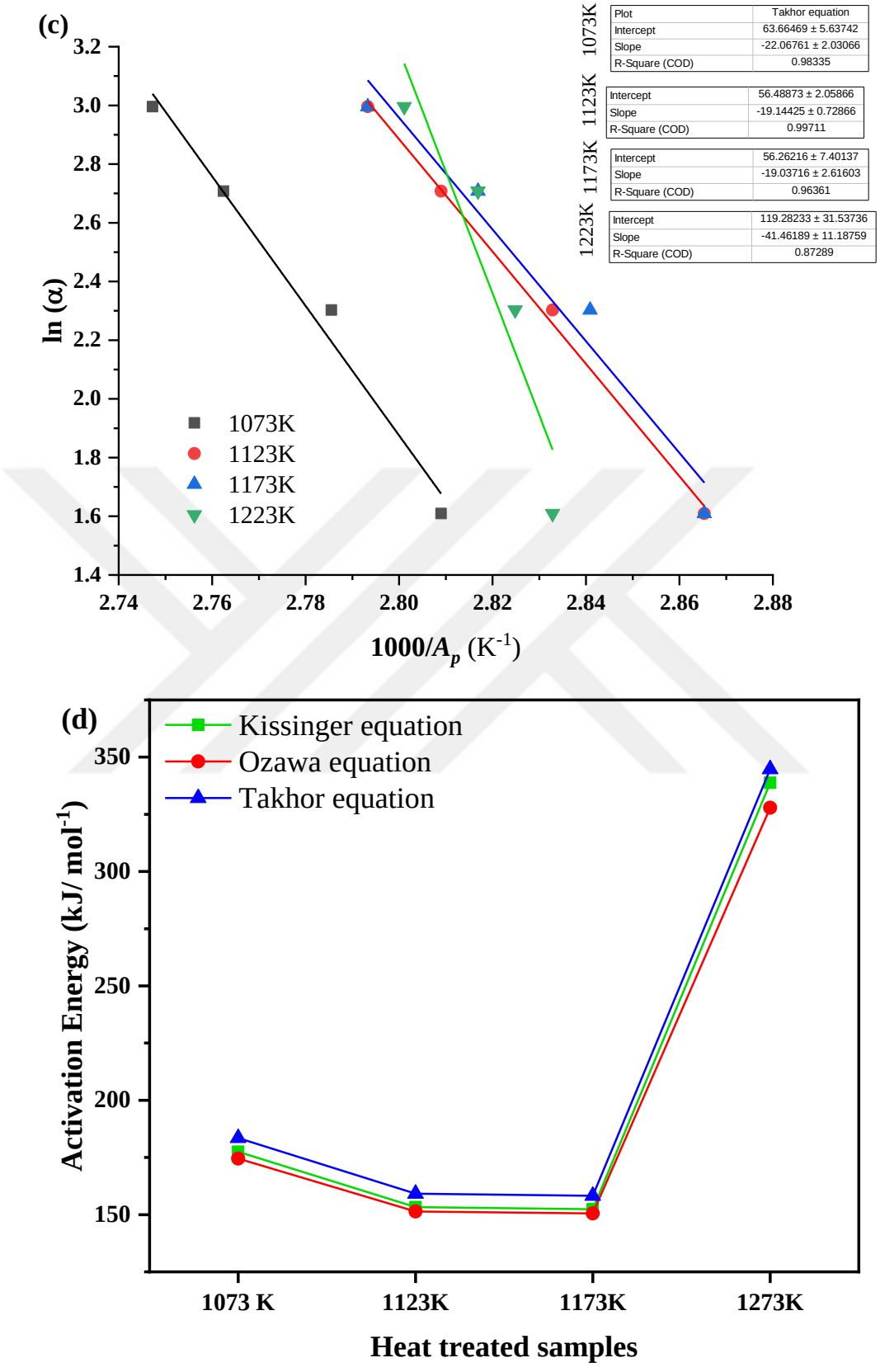

Figure 4.2. Activation energy calculated by (a) Kissinger, (b) Ozawa, and (c) Takhor equations. (d) A comparison between Activation energy as a function of aging temperature (continue)

The calculated E is shown in Figurd. The *E* value is decreased with increasing aging temperature to 1123K (C2), then its value increased by increasing the aging temperature. It is found that the *E* values for nearly equiatomic NiTi [43, 45] and Ni-riched Ni-Ti SMAs [46], are higher than the *E* values of C1, C2, and C3 samples of this study.

Table 4.1 reveals that the PTTs are affected by the thermal cycling process, where the peak of the martensitic phase transformation decreased by increasing the number of cycles. Dilibal et al. [47] found that the austenite phase transformations of NiTiCu SMA were less than Ni-riched NiTi alloys. It can be said that our samples can be classified as Class I SMAs because the martensite starts value is less than austenite start temperature, which is another information that achieved from the DSC and the value of phase transformation temperatures [48].

Table 4.1. Phase transformation temperatures and latent heat of transformation (enthalpy change).

Heating/Cooling Rate (K/min)	**Sample**	A_s **(K)**	A_p **(K)**	A_f **(K)**	M_s **(K)**	M_p **(K)**	M_f **(K)**	ΔH_H **(J/g)**	ΔH_C **(J/g)**
10	C1	348	356	361	342	334	327	8.73	8.72
15		350	359	365	340	332	318	8.11	11.4
20		353	362	370	339	330	319	8.14	9.67
25		356	364	374	338	329	321	7.57	8.78
10	C2	341	349	355	335	326	319	11.5	12
15		344	353	362	333	323	313	11.1	12.8
20		345	356	367	332	321	311	11	12.5
25		347	358	368	332	322	312	12	11.6
10	C3	342	349	356	336	327	320	10.5	11.3
15		344	352	361	334	325	316	10.4	11.6
20		346	355	366	333	324	315	10.5	11.5
25		348	358	369	332	324	315	10.4	10.8
10	C4	349	353	357	344	341	335	1.2	1.24
15		350	354	362	344	339	332	0.93	1.06
20		351	355	362	343	338	331	0.89	1.23
25		353	357	362	342	338	331	1.02	1.08

The phase transformation temperature was obtained from the DSC curves and the data is shown in Figure 4.3. For different heating rates, we can see that the phase transformation temperature was affected, furthermore, the aging temperature influenced the PTTs such that C2 alloy has recorded the lowest PTTs compared to the other specimens. The PTTs are relatively more close to each other in C4 alloy, i.e., the temperature hysteresis of the phase transformation was decreased by the heat treatment process. It is also, reported that composition can influence the temperature hysteresis of NiTiCu alloy [37].

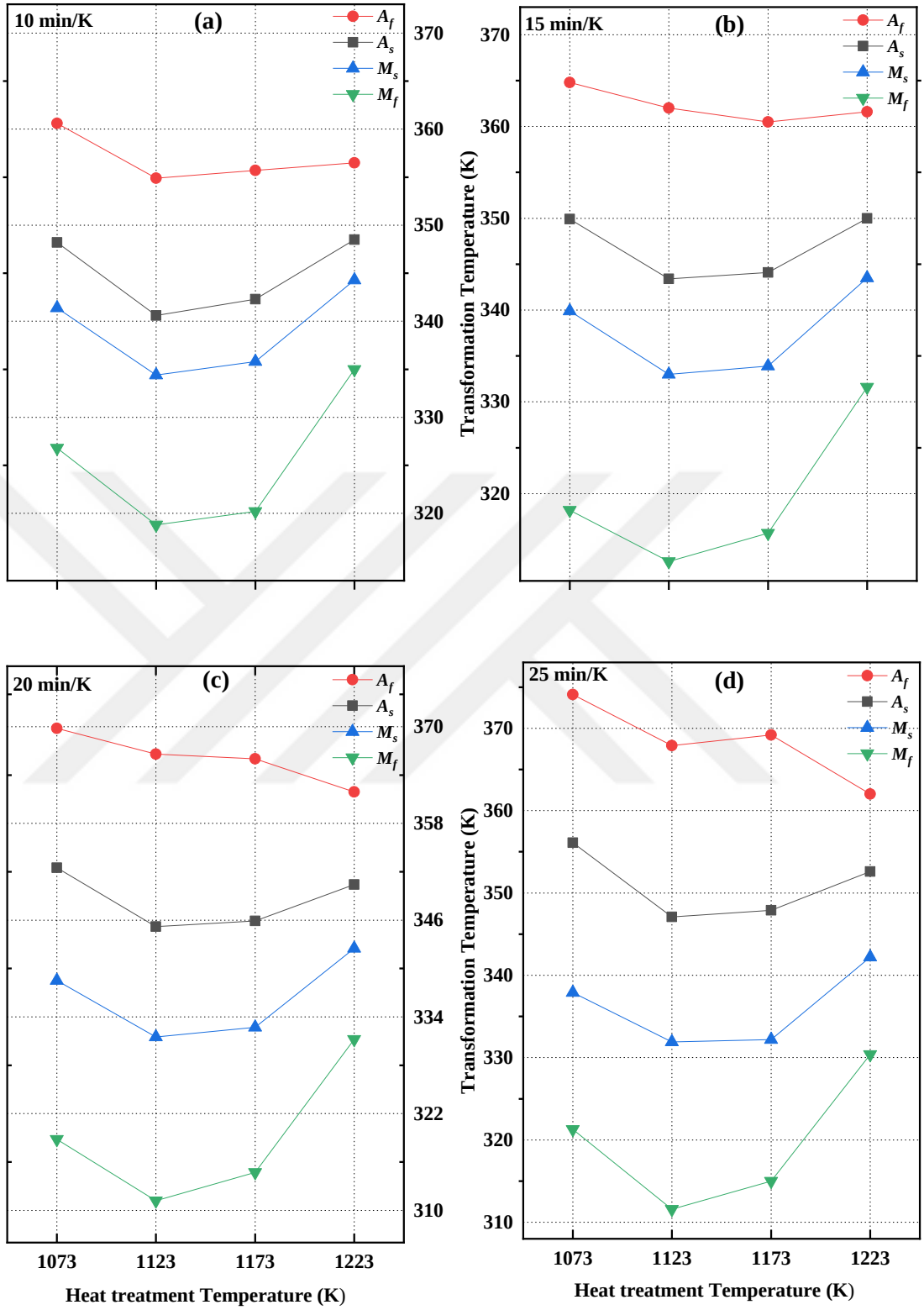

Figure 4.3. The Transformation temperatures of the heat-treated NiTiCu SMAs for different heating rates: (a) 10 min/K, (b) 15 min/K, (c) 20 min/K, and 25 min/K

From the DSC curves, another thermal parameter can be found such as the energy that expelled (exothermic, $\Delta H^{M\rightarrow A}$) or interred (endothermic, $\Delta H^{A\rightarrow M}$) from the samples during phase transformation. As an example, for austenite phase transformation the enthalpy can be formulated as [49]:

$$\Delta H^{M\rightarrow A} = \int_{A_s}^{A_f} \frac{dq}{dt}\left(\frac{dT}{dt}\right)^{-1} dT \tag{4.4}$$

Equation (4.4) is an integration from austenite start to austenite finish that can be changed for exothermic enthalpy change. In the Eq. (4.4) the instantaneous heat gained is represented by (dq/dt); T is the absolute temperature and t is the time. The calculation based on Eq. (4.4) was performed by the DSC software program and the values are listed in Table 4.1. It is worth knowing that the enthalpy change consists of three terms, including internal friction (ΔH_{fr}), chemical energy (ΔH_{ch}), and strain energy (ΔH_{el}) of the transformation. All together as a single value can be obtained by DSC (ΔH_{net}) [50].

Furthermore, entropy change (ΔS) which is the disorderness of microstructural distribution can be found from the total enthalpy change from DSC. The related entropy change be able to calculate from the enthalpy change and the calculated equilibrium temperature ($T_o = (M_s + A_f)/2$) [51, 52]:

$$\Delta S^{M\rightarrow A} = \int_{A_s}^{A_f} \frac{dQ^{M\rightarrow A}}{T_o} = \frac{\Delta H^{M\rightarrow A}}{T_o} \tag{4.5}$$

To calculate the entropy change of the aged NiTiCu alloys, the Eq. (4.5) can be utilized. The obtained results for both forward and reverse transformation is given in Table 4.2. The value of ΔS increased for C2 alloy compared with C1 alloy. By the increasing temperature of aging the entropy change also decreased. Generally, some parameters can affect the entropy change, including the vibrational contribution (ΔS_{vib}), the contribution of the conduction electrons (ΔS_{el}), a magnetic subsystem (ΔS_{mag}), Brillouin zone distortion (ΔS_{dist}), and configuration contributions (ΔS_{conf}) [53-55]. The most of these terms can be discounted, for example, the martensitic phase transformation process is diffusionless thus configuration contributions is equal to zero ($\Delta S_{\mathrm{conf}} = 0$); also the NiTiCu alloy is not a magnetic material, therefore, the magnetic term is also canceled (($\Delta S_{\mathrm{mag}} = 0$)); besides, the electron contribution in the aged SMAs are thought to be equal to zero ($\Delta S_{\mathrm{el}} = 0$); and lastly, the chemical composition is the same, thus electron concentration (e/a) is constant ($\Delta S_{\mathrm{vib}} = 0$). Consequently, the only parameter that can be taken into account is ΔS_{dist}.

Table 4.2. The effect of aging temperature on temperature hysteresis, T_o, $\Delta G^{A\rightarrow M}$, $\Delta S^{A\rightarrow M}$, $\Delta S^{M\rightarrow A}$ and ΔE_e.

Heating/Cooling Rate (K/min.)	Sample	Temperature Hysteresis (K)	T_o (K)	$\Delta G^{A\rightarrow M}$ (J)	$\Delta S^{A\rightarrow M}$ (J/kg.K)	$\Delta S^{M\rightarrow P}$ (J/kg.K)	ΔE_e (J)
10	C1	19	352	236	25	25	372
15		25	353	288	32	23	711
20		31	355	356	27	23	546
25		36	356	383	25	21	419
10	C2	20	345	333	35	33	557
15		29	348	463	37	32	737
20		35	350	551	36	31	751
25		36	350	617	33	34	663
10	C3	20	346	303	33	30	523
15		27	348	404	33	30	601
20		33	350	496	33	30	592
25		37	351	549	31	30	524
10	C4	13	351	22	4	3	32
15		18	353	24	3	3	36
20		19	353	24	3	3	42
25		20	352	29	3	3	34

The Gibbs free energy (ΔG) for reverse phase transformation at equilibrium temperature can be represented as [6, 49]:

$$\Delta G^{M\rightarrow A}(T_o) = G^A(T_o) - G^M(T_o) = (H^A - T_o S^A) - (H^M - T_o S^M)$$
$$= \Delta H^{M\rightarrow A} - (T_o \Delta S^{M\rightarrow A}) = 0 \quad (4.6)$$

where G with superscript *A* and *M* are Gibbs free energy of austenite and martensite phase; *H* and *S* with superscript *A* and *M* denote enthalpy and entropy of the austenite phase. Eq. (4.6) can be simplified as [7, 56]:

$$\Delta G^{A\rightarrow M}(M_s) = \Delta G^{M\rightarrow A}(T_o) - \Delta G^{M\rightarrow A}(M_s) \quad (4.7)$$

or

$$\Delta G^{A\rightarrow M}(M_s) = -(T_o - M_s)\Delta S^{M\rightarrow A} \quad (4.8)$$

The energy stored in martensite variants is called elastic energy (ΔE_e). ΔE_e can be obtained through the subtracting $\Delta G^{A\rightarrow M}$ at two different martensite temperatures (M_s, and M_f) [12, 13, 57]:

$$\Delta E_e = \Delta G^{A\to M}(M_s) - \Delta G^{A\to M}(M_f) = (M_s - M_f)\Delta S^{M\to A} \quad (4.9)$$

The Eq. (4.8) can be substituted into Eq. (4.9), to find the elastic energy for reverse phase transformation:

$$\Delta E_e = (M_s - M_f)\Delta S^{M\to A} \quad (4.10)$$

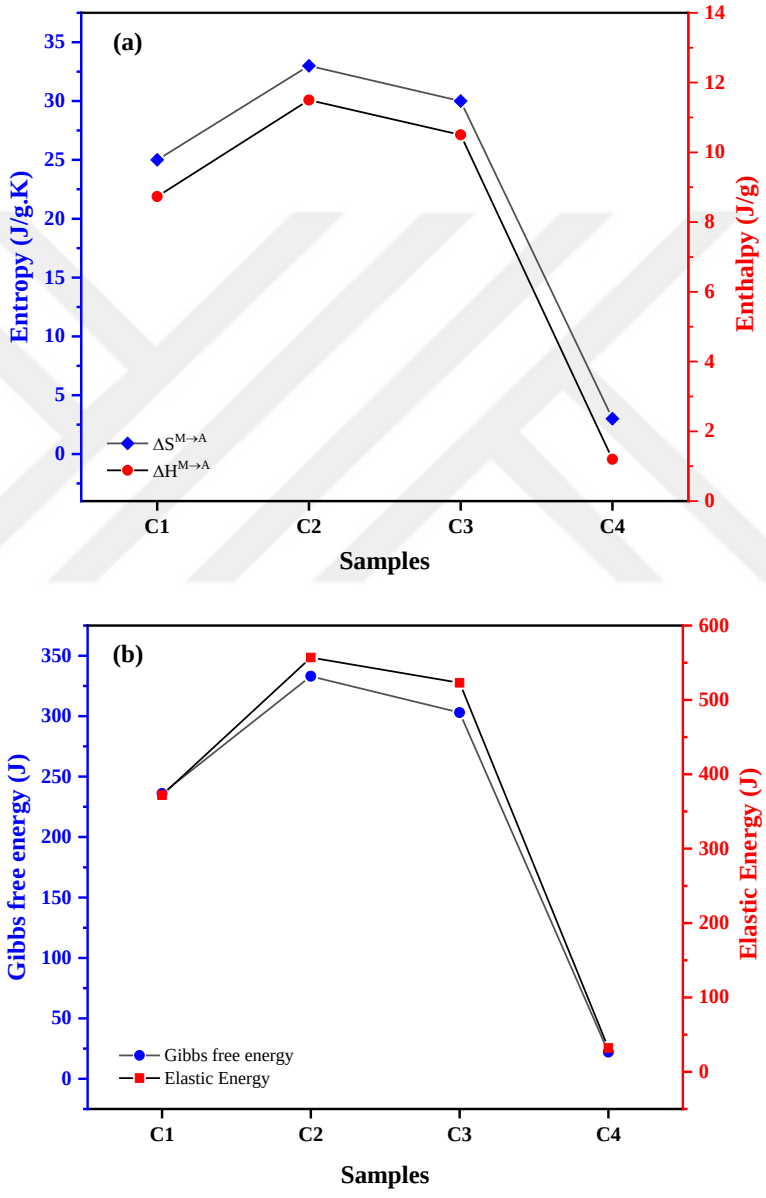

Figure 4.4. (a) Entropy and enthalpy change, (b) Gibbs free energy and elastic energy of the alloys obtained with a heating rate of 10 K/min

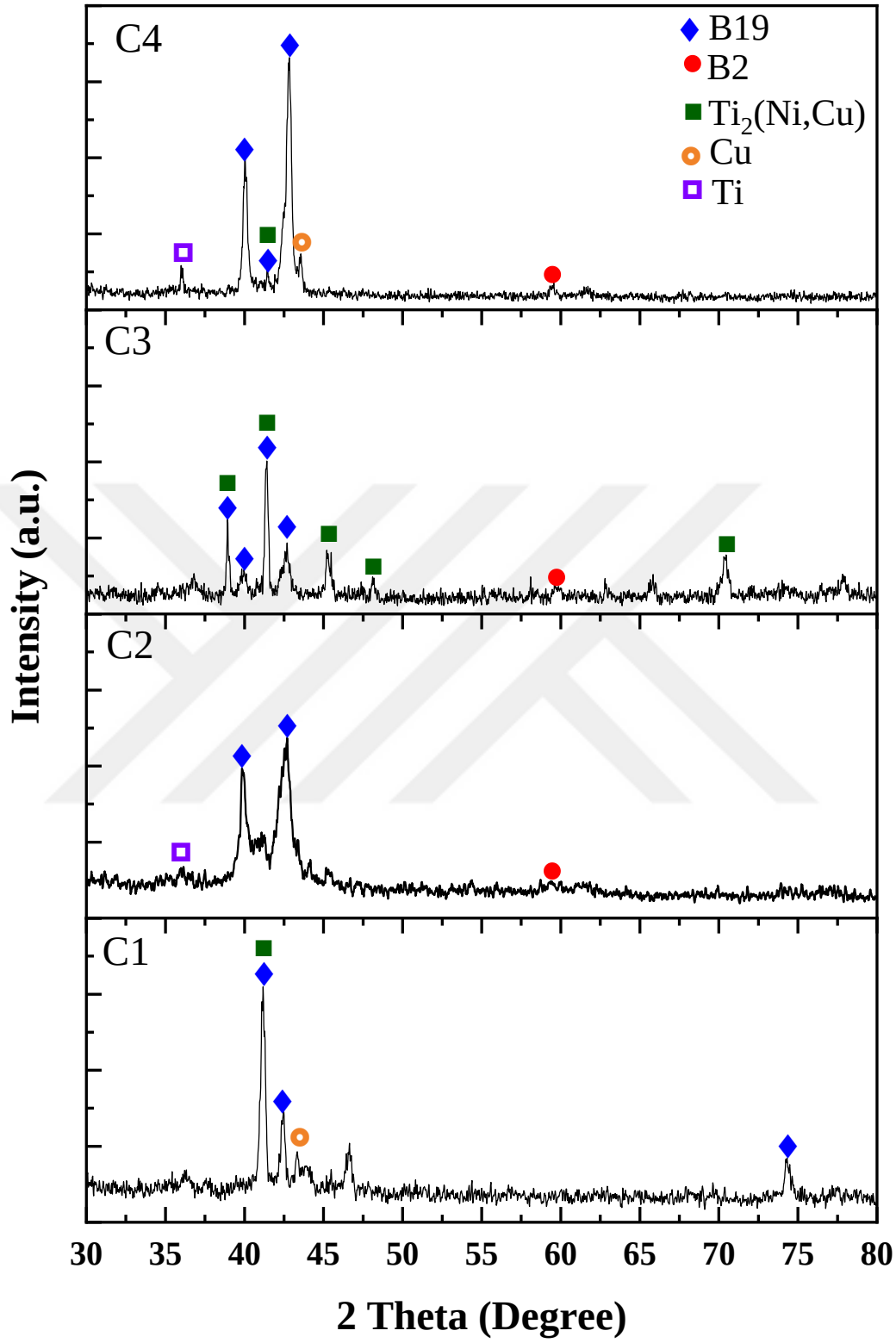

Figure 4.5. The XRD pattern of the NiTiCu SMAs

The obtained value from equations (4.4), (4.5), (4.8) and (4.10) are given in Table 4.2. Figure 4.4 reveals the relationship between enthalpy, entropy (Figure 4.4a), Gibbs free energy, and elastic

energy (Figure 4.4b) with an aging temperature. The alloy, which aged at 1123K, has shown the highest values in all mentioned parameters, and the values reduced with raising the temperature of aging. It can be concluded that the highest enthalpy change specifies that a more portion of the matrix phase was changed during phase transformation [58]. Also, it is reported that the shape memory strain increased with increasing the transition enthalpy [59]. Furthermore, austenite finish temperature (A_f) can increase with increasing time of aging, thus its value directly influences on the entropy change values [60].

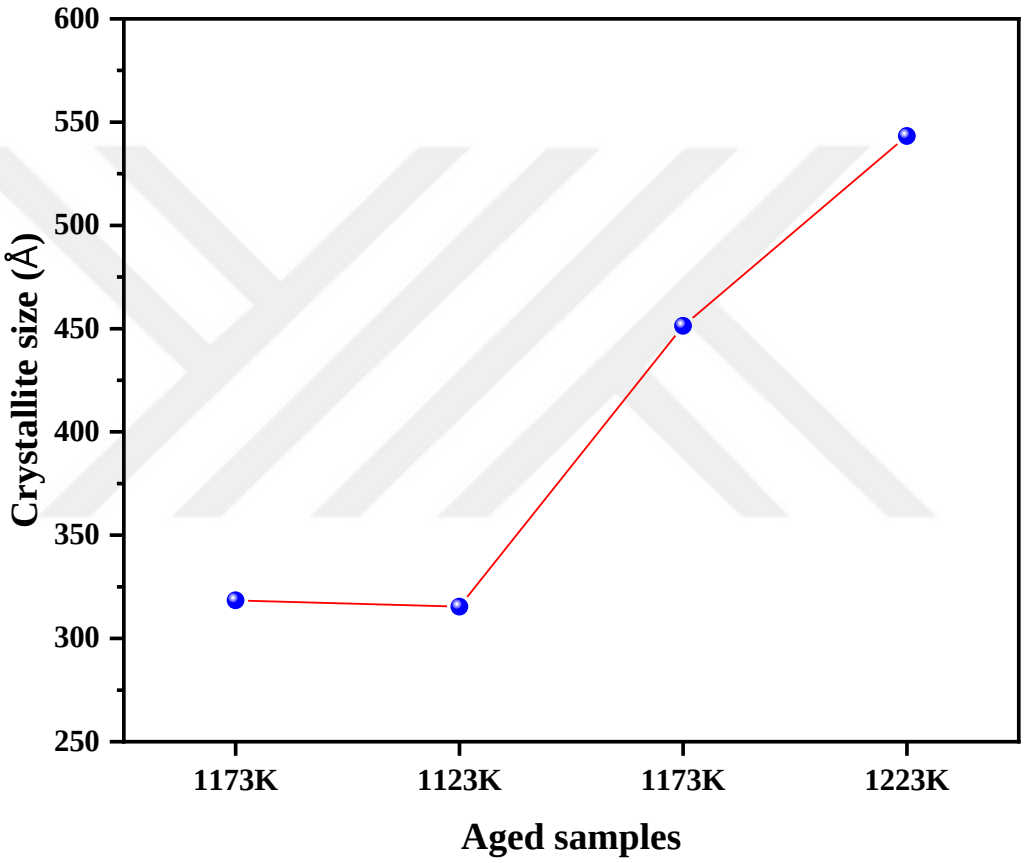

Figure 4.6. The crystallite size of aged NiTiCu SMAs.

Figure 4.5 shows the x-ray diffraction of the aged NiTiCu alloys obtained at room temperature. The XRD peaks were indexed by using literature [61-63]. It shows that the B19 phase is the main phase that denotes the matrix in all SMAs. It can be noticed that only a small fraction of austenite phase (B2) has not completely transferred into the martensite phase. Besides, some peaks represented the Ti_2(Ni, Cu) phase. These precipitations detected in C3 alloy. Another change that can be seen is the pattern and the intensity of the peaks that directly were affected by the changing temperature of aging. Cu elements can be mostly dissolved in the matrix of the alloys.

Also, the XRD pattern gives another information about the crystallite size of the alloys. The Scherrer equation gives the crystallite size of alloys by using XRD pattern [64, 65]:

$$D = K\,\lambda/(B\cos\theta) \tag{4.11}$$

where, *D*, *B*, and θ denote crystallite size, wideness at half maximum (FWHM), and Bragg's angle, respectively; the value chosen for shape factor was (K= 0.9), and the wavelength of the x-ray source was ($\lambda_{K_\alpha}(Cu)$ =1.5406 Å). The calculated crystalline size was the same in both 1073K and 1223K, whereas it grew sharply by increasing the aging temperature (Figure 4.6). The lattice strain diminished by growing the crystallite size [66], which means the elastic energy of the alloy decreased (Figure 4.4b).

Table 4.3. The chemical composition obtained for the aged NiTiCu SMA. The spectrums are the determined regions on the SEM images.

Alloys code	Spectrum no	Ni (%at.)	Ti (%at.)	Cu (%at.)
1073K	1	26.68	52.23	21.10
	2	29.97	51.27	18.76
	3	28.84	51.55	19.64
	4	25.70	51.84	22.47
1123K	1	26.22	52.13	21.65
	2	38.19	52.29	9.52
	3	24.62	53.93	21.45
	4	26.66	52.29	21.05
1173K	1	36.48	46.42	17.11
	2	31.07	49.18	19.75
	3	34.64	50.50	14.86
	4	36.78	50.06	13.15
1223K	1	27.13	52.71	20.16
	2	28.89	49.89	21.21
	3	27.99	50.26	21.72
	4	29.19	50.82	19.99

The optical images obtained from the metallurgical microscope and SEM images taken from a scanning electron microscope are demonstrated in

Figure 4.7 and Figure 4.8. It can be seen that on the surface of the alloys, there are needle-shaped microstructures that represent martensite plates. The SEM images were obtained for a 500x magnification level. Also, the energy dispersive x-ray spectroscopy patterns (Figure 4.8) tells the existence of all constituents used for producing alloy (Ti, Ni, and Cu). In Table 4.3, the quantitative amount for each element was represented, where in most cases we found that the composition is nearly the same as the composition of the as-produced alloy. Additionally, the Ti_3Ni_4 phase was not observed, which is responsible for the two-step phase transformation in DSC results. Also, the

R-phase did not observe in any of EDS and XRD patterns, which showed why the DSC exhibited a single phase transformation between B2 and B19 in all cases [36].

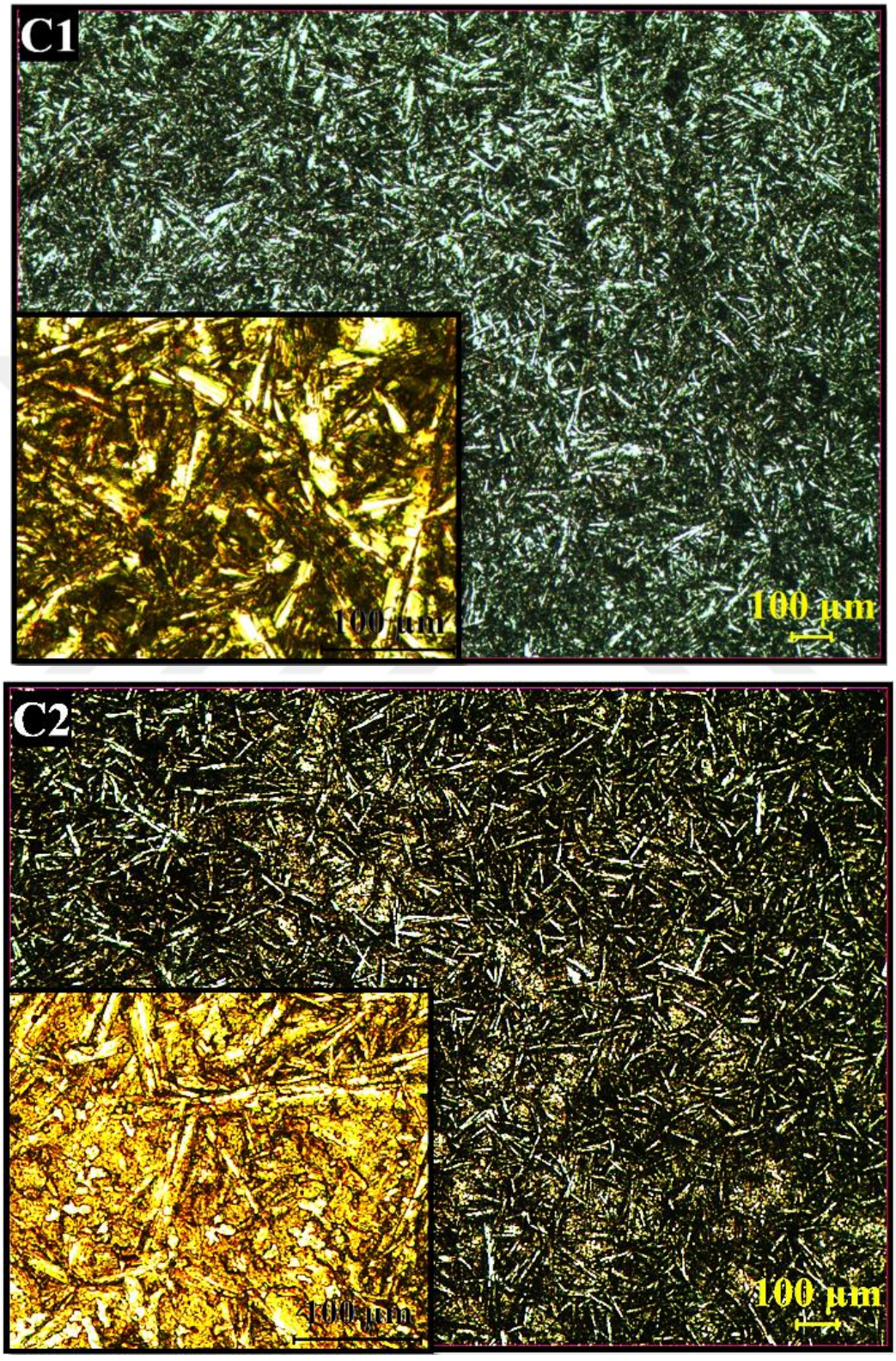

Figure 4.7. The optical microscope images of the as-aged NiTiCu SMA in different aging temperatures

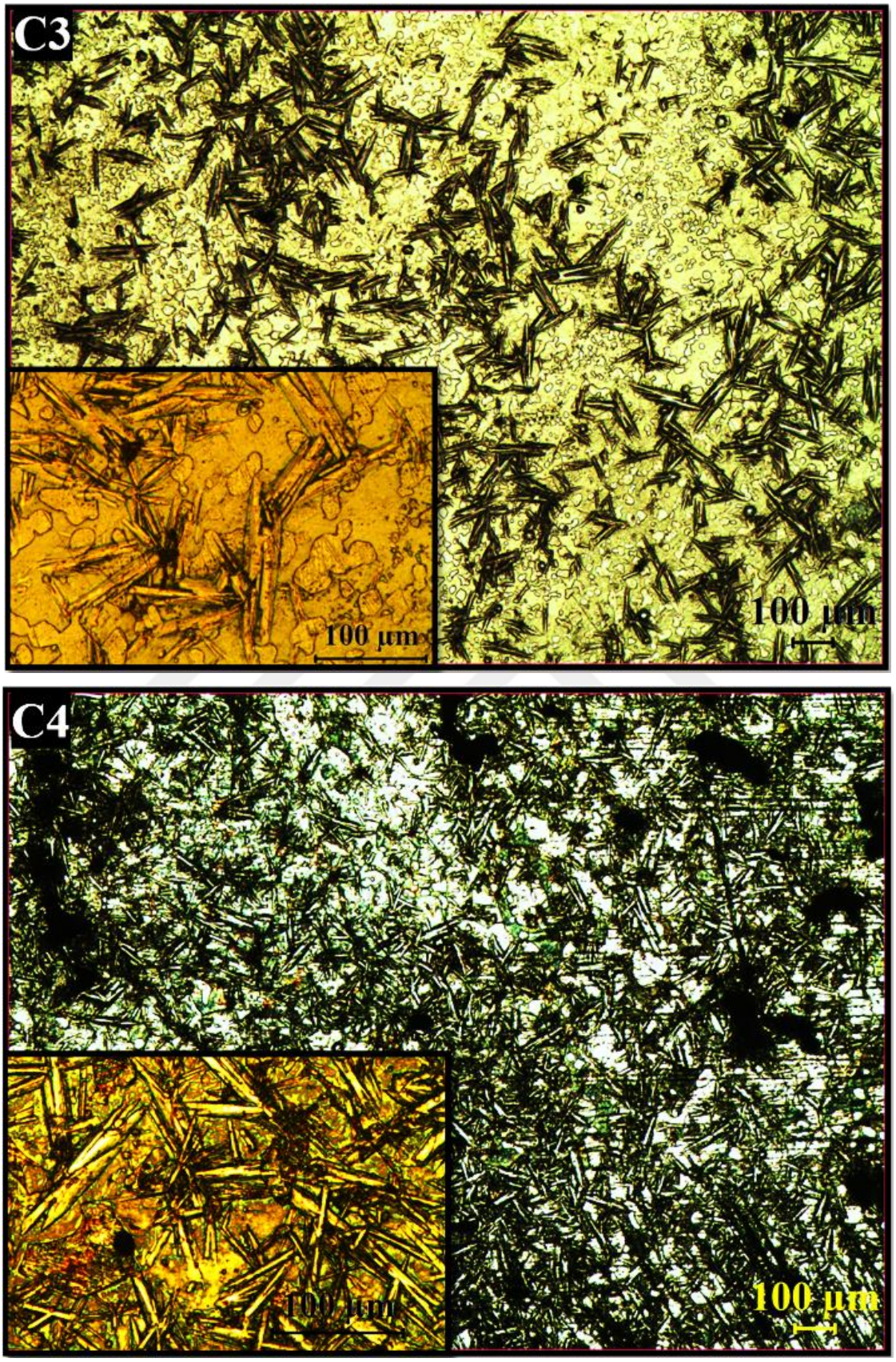

Figure 4.7. The optical microscope images of the as-aged NiTiCu SMA in different aging temperatures (continue)

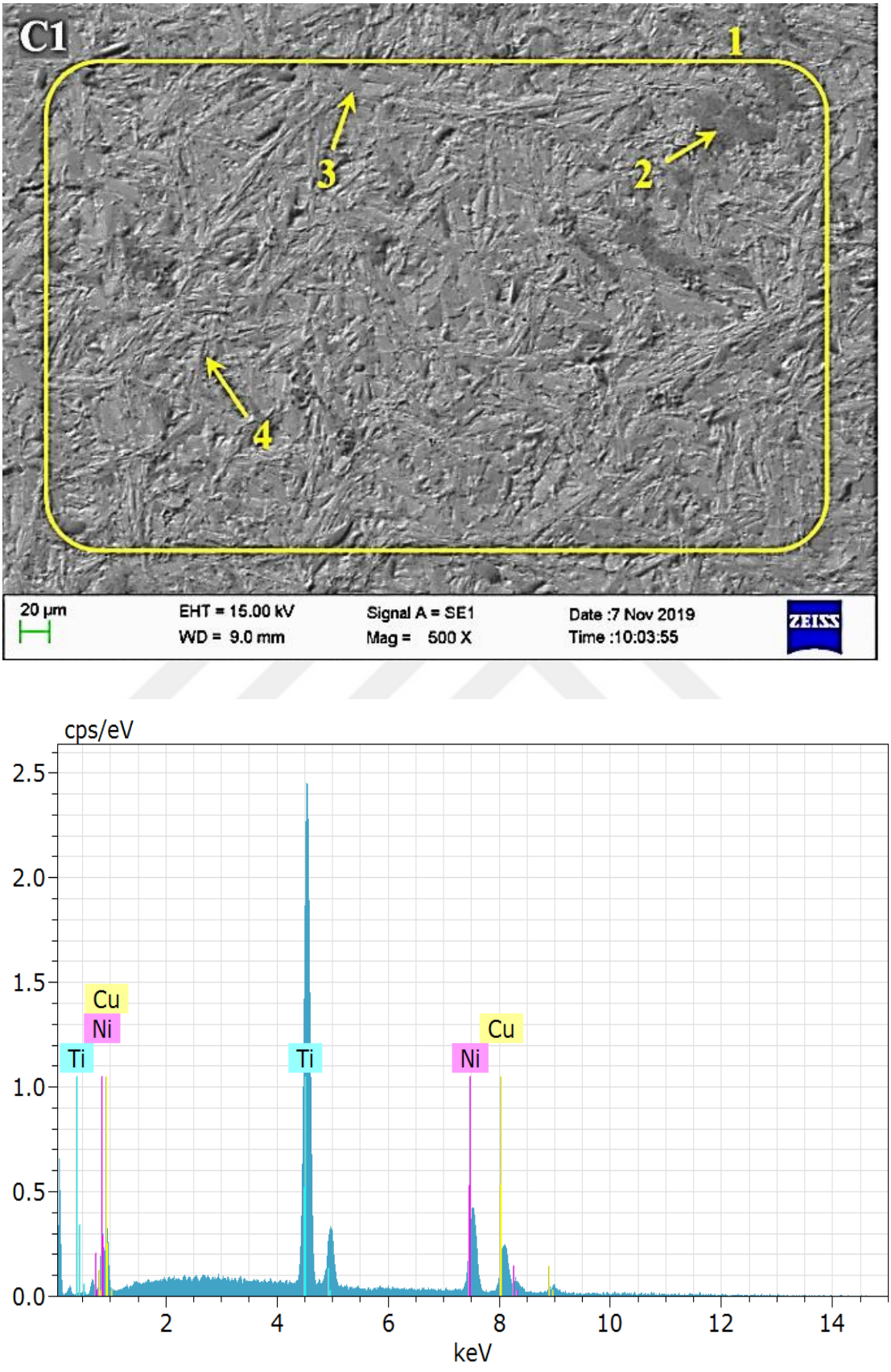

Figure 4.8. The SEM and EDS obtained for the aged NiTiCu alloys

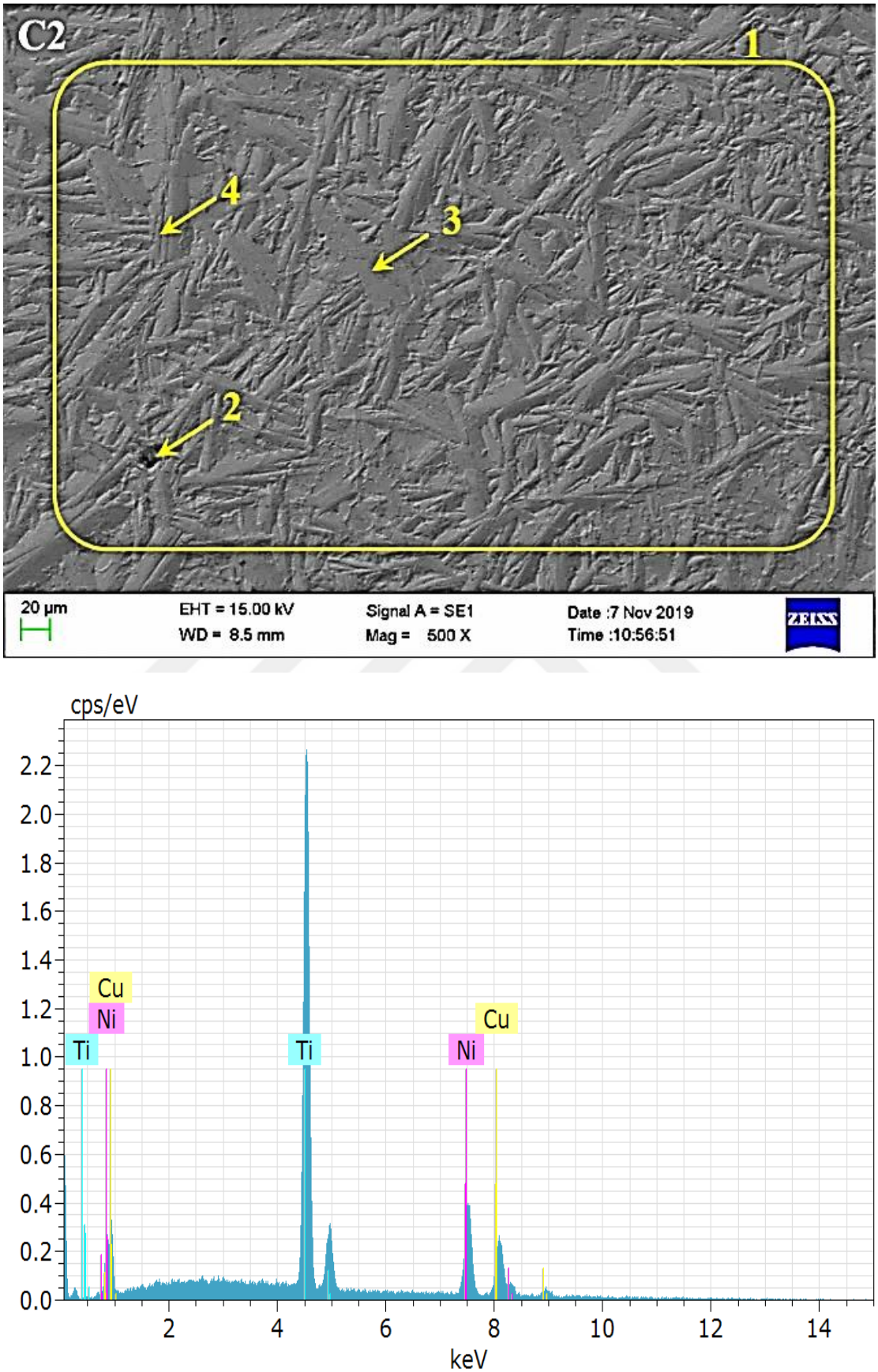

Figure 4.8. The SEM and EDS obtained for the aged NiTiCu alloys (continue)

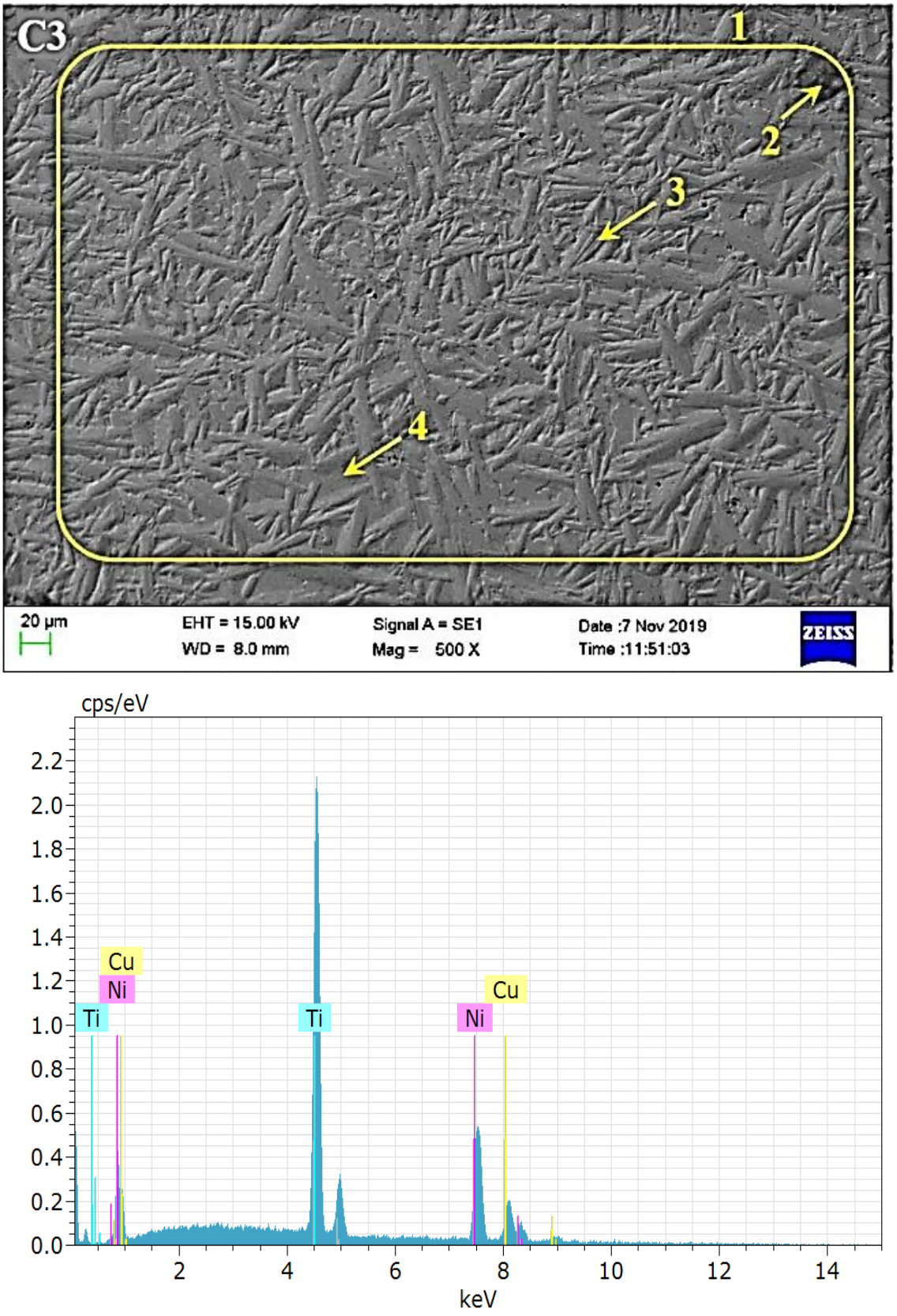

Figure 4.8. The SEM and EDS obtained for the aged NiTiCu alloys (continue).

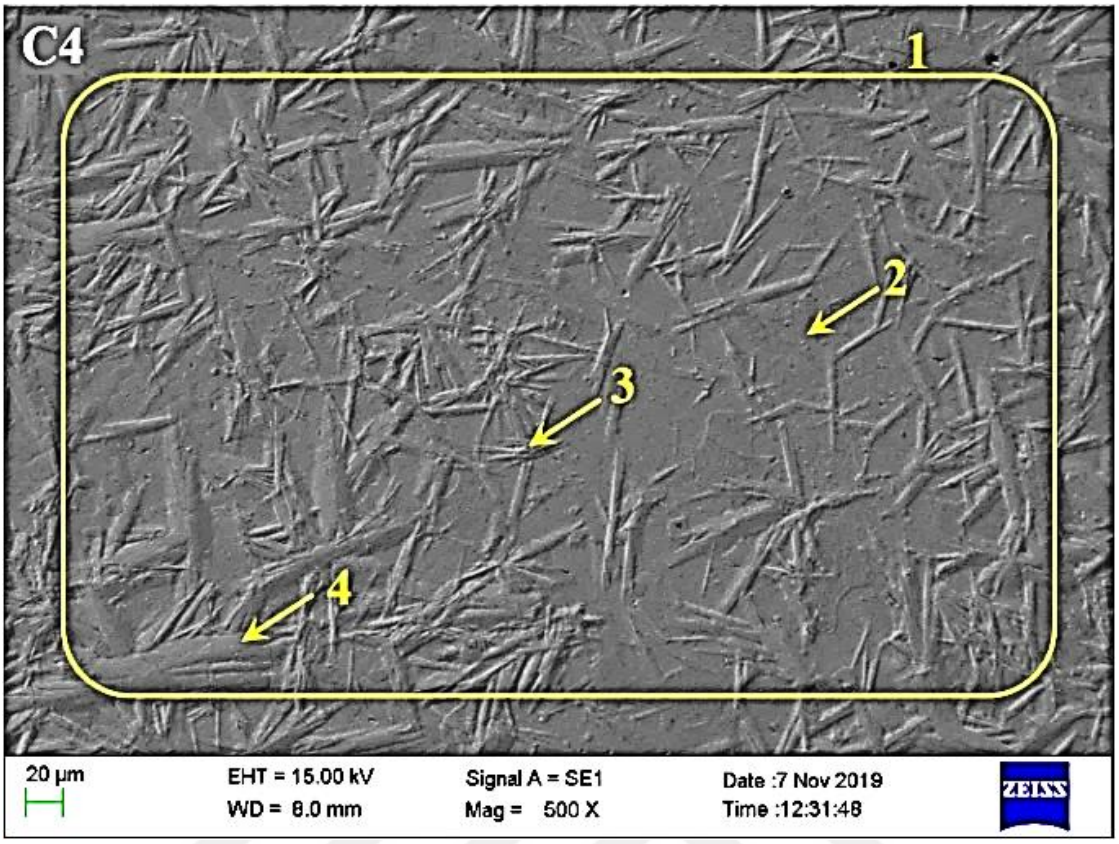

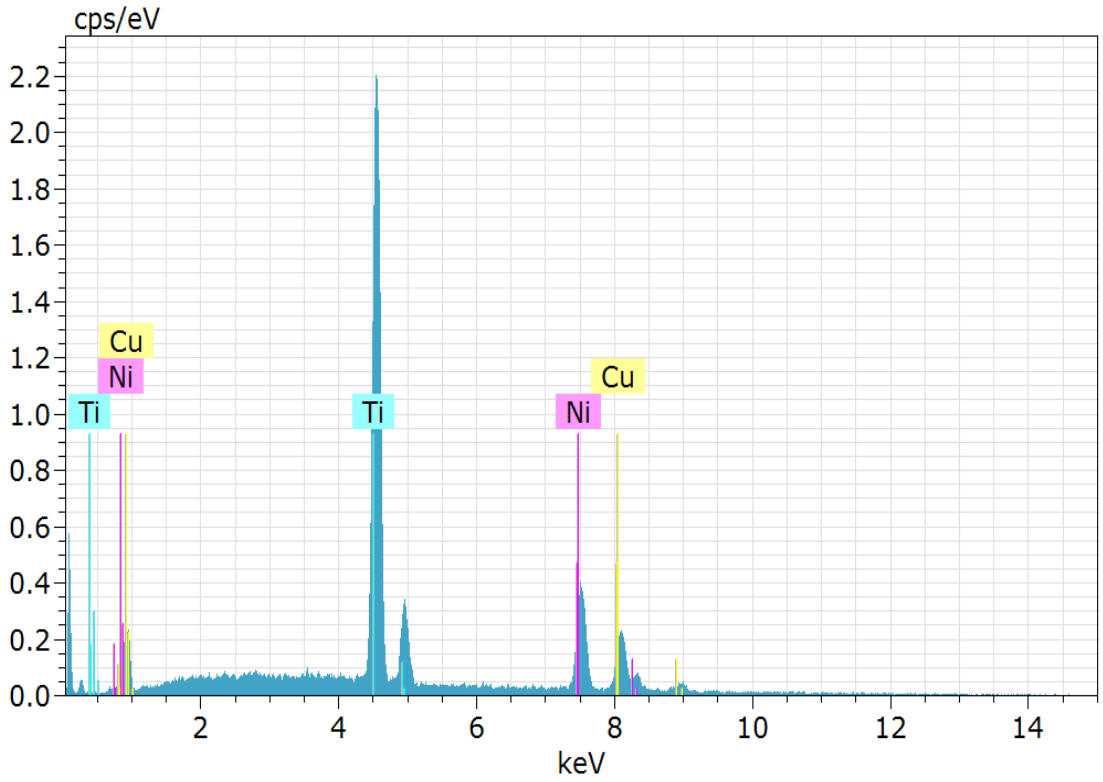

Figure 4.8. The SEM and EDS obtained for the aged NiTiCu alloys (continue).

Figure 4.9 displays the Vickers microhardness outcomes of the aged SMAs. The noticeable change was not observed in the hardness of the alloys, but it can be seen that the second phase recorded a higher value compared to the matrix. It is stated that copper can raise the hardness of NiTi-based SMA [47]. Also, copper can dissolve in the α-Ti, thus the hardness of the alloy can be increased.

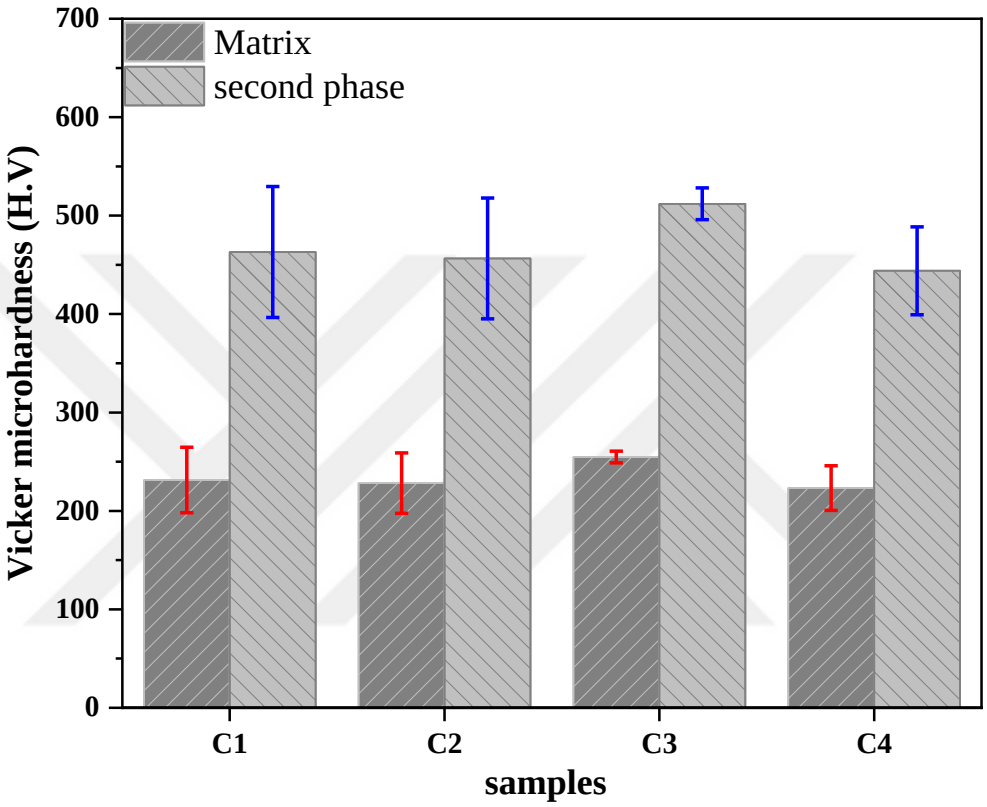

Figure 4.9. The Vickers microhardness of the matrix and the second phase of the aged NiTiCu SMA.

5. CONCLUSION

In this study, a NiTiCu shape memory alloy with a high copper was manufactured by an arc melting device in an argon gas atmosphere. Some pieces were cut from as-quenched alloy and were aged at some determined temperatures. Then the mechanical, thermal, and microstructure of the specimens were studied. In the following bullet point, we have summarized the important outcomes of this study:

- The DSC result displayed that the SMAs can be utilized as low-temperature shape memory alloys. Also, the phase transformation was a single step phase transformation for the measured range of temperatures. The transformation has occurred for B2 ↔ B19.
- The calculated activation energy was reduced by raising the aging temperature to 1173 K (900 ℃). After that, the activation energy sharply increased in C4 aged at 1223 K (950 ℃).
- The C2 had the highest value in enthalpy and entropy change, Gibbs free energy, and elastic energy. The highest enthalpy change, tells that more percentage of the matrix changes during martensitic phase transformation.
- The calculated crystallite size was around 320nm for C1 and C2 alloys, while it increased to about 450 and 550 nm for C3 and C4, respectively.
- In the high-temperature aging, the hardness of the NiTiCu alloys has not considerably affected. The outcomes presented that the hardness of B19 (matrix) was fewer than Ti_2(Ni, Cu) precipitated phase.

RECOMMENDATIONS

The aim of studying for a master's degree in this thesis is to increase the level of my education and my certification is of benefit to the next generation .. because the specialization in physics is a useful discipline and want with our days .. in look of the scientists and specialists who are interested in this field and their follow-up and their interests to form new information about this specialty.

REFERENCES

[1] Es-Souni, M., Es-Souni, M., and Fischer-Brandies, H. (2005). Assessing the biocompatibility of NiTi shape memory alloys used for medical applications, *Analytical and Bioanalytical Chemistry*, C Vol. 381 (3), pp: 557-567. doi: https://doi.org/10.1007/s00216-004-2888-3.

[2] Jani, J.M., Leary, M., Subic, A., and Gibson, M.A. (2014). A review of shape memory alloy research, applications and opportunities, *Materials & Design (1980-2015)*, C Vol. 56 1078-1113.

[3] Saadat, S., Salichs, J., Noori, M., Hou, Z., Davoodi, H., Bar-On, I., Suzuki, Y., and Masuda, A. (2002). An overview of vibration and seismic applications of NiTi shape memory alloy, *Smart Materials and Structures*, C Vol. 11 (2), pp: 218.

[4] Ercan, E., Dagdelen, F., and Qader, I. (2020). Effect of tantalum contents on transformation temperatures, thermal behaviors and microstructure of CuAlTa HTSMAs, *Journal of Thermal Analysis and Calorimetry*, C Vol. 139 (1), pp: 29-36. doi: https://doi.org/10.1007/s10973-019-08418-y.

[5] Kök, M., Zardawi, H.S.A., Qader, I.N., and Kanca, M.S. (2019). The effects of cobalt elements addition on Ti2Ni phases, thermodynamics parameters, crystal structure and transformation temperature of NiTi shape memory alloys, *The European Physical Journal Plus*, C Vol. 134 (5), pp: 197. doi: https://doi.org/10.1140/epjp/i2019-12570-9.

[6] Dagdelen, F., Kok, M., and Qader, I. (2019). Effects of Ta Content on Thermodynamic Properties and Transformation Temperatures of Shape Memory NiTi Alloy, *Metals and Materials International*, C Vol. 1420–1427. doi: https://doi.org/10.1007/s12540-019-00298-z.

[7] Dagdelen, F., Esra, B., Qader, I.N., Ozen, E., Kok, M., Kanca, M.S., Abdullah, S.S., and Mohammed, S.S. (2020). Influence of the Nb Content on the Microstructure and Phase Transformation Properties of NiTiNb Shape Memory Alloys, *JOM*, C Vol. 72 1664–1672. doi: https://doi.org/10.1007/s11837-020-04026-6.

[8] Buytoz, S., Dagdelen, F., Qader, I., Kok, M., and Tanyildizi, B. (2019). Microstructure Analysis and Thermal Characteristics of NiTiHf Shape Memory Alloy with Different Composition, *Metals and Materials International*, C Vol. 1-12. doi: https://doi.org/10.1007/s12540-019-00444-7.

[9] Kumar, P., Jain, A.K., Hussain, S., Pandey, A., and Dasgupta, R. (2015). Changes in the properties of Cu-Al-Mn shape memory alloy due to quaternary addition of different elements, *Matéria (Rio de Janeiro)*, C Vol. 20 (1), pp: 284-292.

[10] Elahinia, M.H., Hashemi, M., Tabesh, M., and Bhaduri, S.B. (2012). Manufacturing and processing of NiTi implants: a review, *Progress in Materials Science*, C Vol. 57 (5), pp: 911-946.

[11] Thierry, B., Tabrizian, M., Trepanier, C., Savadogo, O., and Yahia, L.H. (2000). Effect of surface treatment and sterilization processes on the corrosion behavior of NiTi shape memory alloy, *Journal of Biomedical Materials Research*, C Vol. 51 (4), pp: 685-693.

[12] Qader, I.N., Kök, M., and Dağdelen, F. (2019). Effect of heat treatment on thermodynamics parameters, crystal and microstructure of (Cu-Al-Ni-Hf) shape memory alloy, *Physica B: Condensed Matter*, C Vol. 553 1-5. doi: https://doi.org/10.1016/j.physb.2018.10.021.

[13] Kok, M., Al-Jaf, A.O.A., Çirak, Z.D., Qader, I.N., and Özen, E. (2020). Effects of heat treatment temperatures on phase transformation, thermodynamical parameters, crystal microstructure, and electrical resistivity of NiTiV shape memory alloy, *Journal of Thermal Analysis and Calorimetry*, C Vol. 139 3405–3413. doi: https://doi.org/10.1007/s10973-019-08788-3.

[14] Dagdelen, F., Aldalawi, M.A.K., Kok, M., and Qader, I.N. (2019). Influence of Ni addition and heat treatment on phase transformation temperatures and microstructures of a ternary CuAlCr alloy, *The European Physical Journal Plus*, C Vol. 134 (2), pp: 66. doi: https://doi.org/10.1140/epjp/i2019-12479-3.

[15] Fabregat-Sanjuan, A., Ferrando, F., and De la Flor, S. (2014). NiTiCu shape memory alloy characterization through microhardness tests, *Journal of Materials Engineering and Performance*, C Vol. 23 (7), pp: 2498-2504. doi: https://doi.org/10.1007/s11665-014-1099-0.

[16] Tatar, C., Acar, R., and Qader, I.N. (2020). Investigation of thermodynamic and microstructural characteristics of NiTiCu shape memory alloys produced by arc-melting method, *The European Physical Journal Plus*, C Vol. 135 311. doi: https://doi.org/10.1140/epjp/s13360-020-00288-w.

[17] Fabregat-Sanjuan, A., Ferrando, F., and De la Flor, S. (2015). Influence of heat treatment on internal friction spectrum in NiTiCu shape memory alloy, *Materials Today: Proceedings*, C Vol. 2 S755-S758.

[18] Shi, P., Yang, D., Shen, H., and Chen, F. (2000). Effects of aging on martensitic transformation of Ti50Ni25Cu25 shape memory alloy, *Materials & Design*, C Vol. 21 (6), pp: 521-524. doi: https://doi.org/10.1016/S0261-3069(00)00009-1.

[19] Nespoli, A. and Besseghini, S. (2011). A complete thermo-mechanical study of a NiTiCu shape memory alloy wire, *Journal of Thermal Analysis and Calorimetry*, C Vol. 103 (3), pp: 821-826. doi: https://doi.org/10.1007/s10973-010-1042-z.
[20] AbuZaiter, A., Ng, E.L., Kazi, S., Ali, M., and Sultan, M. (2015). Development of miniature stewart platform using TiNiCu shape-memory-alloy actuators, *Advances in Materials Science and Engineering*, C Vol. 2015. doi: https://doi.org/10.1155/2015/928139.
[21] Jafer, T.A.O., (2017). *Studying the Crystalline Structure of Materials Using X-ray Diffraction*, *Sudan University of Science and Technology*. Ph.D. thesis,
[22] Chekotu, J.C., Groarke, R., O'Toole, K., and Brabazon, D. (2019). Advances in Selective Laser Melting of Nitinol Shape Memory Alloy Part Production, *Materials*, C Vol. 12 (5), pp: 809.
[23] Vander Voort, G.F., Lampman, S.R., Sanders, B.R., Anton, G.J., Polakowski, C., Kinson, J., Muldoon, K., Henry, S.D., and Scott Jr, W.W. (2004). ASM handbook, *Metallography and microstructures*, C Vol. 9 44073-0002.
[24] Losertová, M., Štencek, M., Matýsek, D., Štefek, O., and Drápala, J. (2017). Microstructure evolution of heat treated NiTi alloys. in *IOP Conference Series: Materials Science and Engineering*. IOP Publishing.
[25] Chen, K.C. (2003). NiTi-Magic or Phase Transformation? in *Proceedings of the ASEE Annual Conference & Exposition: Nashville, TN*.
[26] Milne, D. and Witten, I.H. (2013). An open-source toolkit for mining Wikipedia, *Artificial Intelligence*, C Vol. 194 222-239.
[27] Jiang, S., Yu, J., Hu, L., and Zhang, Y. (2017). Investigation on Deformation Mechanisms of NiTi Shape Memory Alloy Tube under Radial Loading, *Metals*, C Vol. 7 (7), pp: 268. doi: https://doi.org/10.3390/met7070268.
[28] Lampert, N.R., *Optical fiber connection utilizing fiber containing ferrules*, 2005, Google Patents.
[29] Brojan, M., Bombač, D., Kosel, F., and Videnič, T. (2008). Shape memory alloys in medicine, *RMZ-Materials and geoenvironment*, C Vol. 2 (55), pp: 173-189.
[30] Fernandes, D.J., Peres, R.V., Mendes, A.M., and Elias, C.N. (2011). Understanding the shape-memory alloys used in orthodontics, *ISRN dentistry*, C Vol. 2011.
[31] Marattukalam, J.J., Balla, V.K., Das, M., Bontha, S., and Kalpathy, S.K. (2018). Effect of heat treatment on microstructure, corrosion, and shape memory characteristics of laser deposited NiTi alloy, *Journal of alloys and compounds*, C Vol. 744 337-346.
[32] Liu, Q., Ma, X., Lin, C., and Wu, Y. (2006). Effect of the heat treatment on the damping characteristics of the NiTi shape memory alloy, *Materials Science and Engineering: A*, C Vol. 438 563-566.
[33] Bujoreanu, L.-G., Young, M.L., Gollerthan, S., Somsen, C., and Eggeler, G. (2010). Influence of heat treatment and microstructure on the tensile pseudoelastic response of an Ni-rich NiTi shape memory alloy, *International journal of materials research*, C Vol. 101 (5), pp: 623-630.
[34] Wang, X., Caldow, R., Sem, G.J., Hama, N., and Sakurai, H. (2010). Evaluation of a condensation particle counter for vehicle emission measurement: Experimental procedure and effects of calibration aerosol material, *Journal of Aerosol Science*, C Vol. 41 (3), pp: 306-318.
[35] Jiang, S.-y., Zhang, Y.-q., Zhao, Y.-n., Liu, S.-w., Hu, L., and Zhao, C.-z. (2015). Influence of Ni4Ti3 precipitates on phase transformation of NiTi shape memory alloy, *Trans. Nonferrous Met. Soc. China*, C Vol. 25 (4063), pp: 4071. doi: https://doi.org/10.1016/S1003-6326(15)64056-0.
[36] Otsuka, K. and Ren, X. (2005). Physical metallurgy of Ti–Ni-based shape memory alloys, *Progress in Materials Science*, C Vol. 50 (5), pp: 511-678. doi: https://doi.org/10.1016/j.pmatsci.2004.10.001.
[37] Tang, W., Sandström, R., Wei, Z., and Miyazaki, S. (2000). Experimental investigation and thermodynamic calculation of the Ti-Ni-Cu shape memory alloys, *Metallurgical and Materials Transactions A*, C Vol. 31 (10), pp: 2423-2430. doi: https://doi.org/10.1007/s11661-000-0187-y.
[38] Lin, K.-N. and Wu, S.-K. (2010). Multi-stage transformation in annealed Ni-rich Ti49Ni41Cu10 shape memory alloy, *Intermetallics*, C Vol. 18 (1), pp: 87-91. doi: https://doi.org/10.1016/j.intermet.2009.06.011.
[39] Vyazovkin, S. (2016). A time to search: finding the meaning of variable activation energy, *Physical Chemistry Chemical Physics*, C Vol. 18 (28), pp: 18643-18656.
[40] Parmar, D., Sugiono, E., Raja, S., and Rueping, M. (2017). Addition and correction to complete field guide to asymmetric BINOL-phosphate derived Brønsted acid and metal catalysis: History and classification by mode of activation; Brønsted acidity, hydrogen bonding, ion pairing, and metal phosphates, *Chemical reviews*, C Vol. 117 (15), pp: 10608-10620.
[41] Kissinger, H.E. (1957). Reaction kinetics in differential thermal analysis, *Analytical Chemistry*, C Vol. 29 (11), pp: 1702-1706. doi: https://doi.org/10.1021/ac60131a045.

[42] Ozawa, T. (1965). A new method of analyzing thermogravimetric data, *Bulletin of the Chemical Society of Japan*, C Vol. 38 (11), pp: 1881-1886. doi: https://doi.org/10.1246/bcsj.38.1881.
[43] Kaya, I., Özdemir, Y., Kaya, E., and Keskin, M.E. (2019). The heating–cooling rate effect on thermal properties of high nickel-rich NiTi shape memory alloy, *Journal of Thermal Analysis and Calorimetry*, C Vol. 1-6. doi: https://doi.org/10.1007/s10973-019-08511-2.
[44] Takhor, R. Advances in Nucleation and Crystallization of Glasses; American Ceramics Society: Columbus, OH, 1971; p 166, *There is no corresponding record for this reference.[Google Scholar]*, C Vol.
[45] Acar, E. (2016). The determination of the phase transformations and the activation energies in TiNi smart alloys, *Gazi Univ Sci J Part C Des Technol*, C Vol. 4 (3), pp: 165-71.
[46] Dağdelen, F., Buytoz, S., and Akbaş, İ. (2017). The effects on thermal and microstructure properties of Cu addition in NiTi SMAs, *Fırat Univ J Eng Sci*, C Vol. 29 (1), pp: 269-75.
[47] Dilibal, S. and Adanir, H. (2013). Comparison and Characterization of NiTi and NiTiCu Shape Memory Alloys. in *Safety is Not an Option, Proceedings of the 6th IAASS Conference*.
[48] Acar, E., Kok, M., and Qader, I. (2020). Exploring surface oxidation behavior of NiTi–V alloys, *The European Physical Journal Plus*, C Vol. 135 (1), pp: 58. doi: https://doi.org/10.1140/epjp/s13360-019-00087-y.
[49] Kök, M., Qader, I.N., Mohammed, S.S., ÖNER, E., Dağdelen, F., and Aydogdu, Y. (2020). Thermal Stability and Some Thermodynamics Analysis of Heat Treated Quaternary CuAlNiTa Shape Memory Alloy, *Materials Research Express*, C Vol. 7. doi: https://doi.org/10.1088/2053-1591/ab5bef.
[50] Li, B.-Y., Rong, L.-J., Luo, X.-H., and Li, Y.-Y. (1999). Transformation behavior of sintered porous NiTi alloys, *Metallurgical and Materials Transactions A*, C Vol. 30 (11), pp: 2753-2756. doi: https://doi.org/10.1007/s11661-999-0112-y.
[51] Elrasasi, T., Dobróka, M., Daróczi, L., and Beke, D. (2013). Effect of thermal and mechanical cycling on the elastic and dissipative energy in CuAl (11.5 wt%) Ni (5.0 wt%) shape memory alloy, *Journal of alloys and compounds*, C Vol. 577 S517-S520.
[52] Ozgen, S. and Tatar, C. (2012). Thermoelastic transition kinetics of a gamma irradiated CuZnAl shape memory alloy, *Metals and Materials International*, C Vol. 18 (6), pp: 909-916.
[53] Romero, R. and Pelegrina, J. (1994). Entropy change between the β phase and the martensite in Cu-based shape-memory alloys, *Physical Review B*, C Vol. 50 (13), pp: 9046. doi: https://doi.org/10.1103/PhysRevB.50.9046.
[54] Khovailo, V., Oikawa, K., Abe, T., and Takagi, T. (2003). Entropy change at the martensitic transformation in ferromagnetic shape memory alloys Ni 2+ x Mn 1− x Ga, *Journal of Applied Physics*, C Vol. 93 (10), pp: 8483-8485. doi: https://doi.org/10.1063/1.1556218.
[55] Romero, R. and Pelegrina, J. (2003). Change of entropy in the martensitic transformation and its dependence in Cu-based shape memory alloys, *Materials Science and Engineering: A*, C Vol. 354 (1-2), pp: 243-250. doi: https://doi.org/10.1016/S0921-5093(03)00013-3.
[56] Dagdelen, F., Gokhan, T., Aydogdu, A., Aydogdu, Y., and Adigüzel, O. (2003). Effects of thermal treatments on transformation behaviour in shape memory Cu–Al–Ni alloys, *Materials Letters*, C Vol. 57 (5-6), pp: 1079-1085.
[57] Tatar, C., Yildirim, Z., and Kaygili, O. (2017). Effect of Hydrostatic Pressure on Thermodynamic Properties of NiTi Shape Memory Alloy, *Archives of Metallurgy and Materials*, C Vol. 62 (2), pp: 799-806.
[58] Kaya, M., Çakmak, Ö., Gülenç, B., and Atlı, K.C. (2017). Thermomechanical cyclic stability of porous NiTi shape memory alloy, *Materials Research Bulletin*, C Vol. 95 243-247. doi: https://doi.org/10.1016/j.materresbull.2017.07.016.
[59] Kaya, M. and Çakmak, Ö. (2016). Shape Memory behavior of porous NiTi alloy, *Metallurgical and Materials Transactions A*, C Vol. 47 (4), pp: 1499-1503. doi: https://doi.org/10.1007/s11661-015-3318-1.
[60] ERCAN, E., DAĞDELEN, F., Mediha, K., and BALCI, E. Investigation of Thermodynamic Properties of Ni30Ti20Cu20 Shape Memory Alloy, *Bitlis Eren Üniversitesi Fen Bilimleri Dergisi*, C Vol. 8 (4), pp: 1194-1202.
[61] Yang, C., Cheng, Q., Liu, L., Li, Y., and Li, Y. (2015). Effect of minor Cu content on microstructure and mechanical property of NiTiCu bulk alloys fabricated by crystallization of metallic glass powder, *Intermetallics*, C Vol. 56 37-43. doi: https://doi.org/10.1016/j.intermet.2014.08.009.
[62] Morakabati, M., Kheirandish, S., Aboutalebi, M., Taheri, A.K., and Abbasi, S. (2010). The effect of Cu addition on the hot deformation behavior of NiTi shape memory alloys, *Journal of alloys and compounds*, C Vol. 499 (1), pp: 57-62. doi: https://doi.org/10.1016/j.jallcom.2010.01.124.

[63] Maleksaeedi, S., Wang, J.K., El-Hajje, A., Harb, L., Guneta, V., He, Z., Wiria, F.E., Choong, C., and Ruys, A.J. (2013). Toward 3D printed bioactive titanium scaffolds with bimodal pore size distribution for bone ingrowth, *Procedia CIRP*, C Vol. 5 (0), pp: 158-163. doi: https://doi.org/10.1016/j.procir.2013.01.032.

[64] Saud, S.N., Hamzah, E., Abubakar, T., Zamri, M., and Tanemura, M. (2014). Influence of Ti additions on the martensitic phase transformation and mechanical properties of Cu–Al–Ni shape memory alloys, *Journal of Thermal Analysis and Calorimetry*, C Vol. 118 (1), pp: 111-122.

[65] Patterson, A. (1939). The Scherrer formula for X-ray particle size determination, *Physical Review*, C Vol. 56 (10), pp: 978.

[66] Velmurugan, C. and Senthilkumar, V. (2018). The effect of Cu addition on the morphological, structural and mechanical characteristics of nanocrystalline NiTi shape memory alloys, *Journal of alloys and compounds*, C Vol. 767 944-954. doi: https://doi.org/10.1016/j.jallcom.2018.07.217.

CURRICULUM VITAE

Azad Ibrahim HAJI

PERSONAL INFORMATION

[redacted]

RESEARCH EXPERIENCES

- ✓ DSC, TGA, DTA
- ✓ Computer programs (MS word, MS excel, MS powerpoint)

WORK EXPERIENCE

2015 –2020: Education and teaching